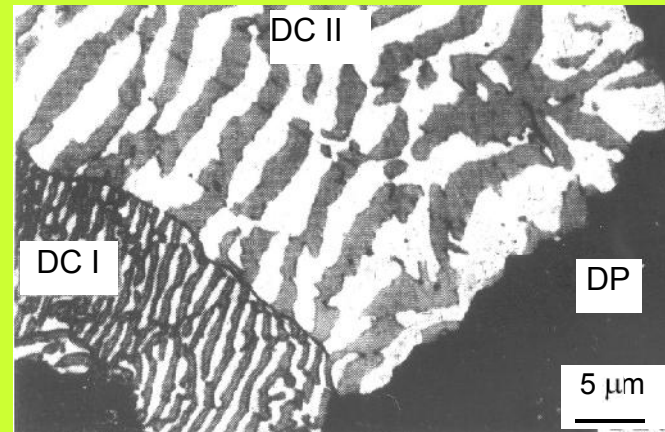
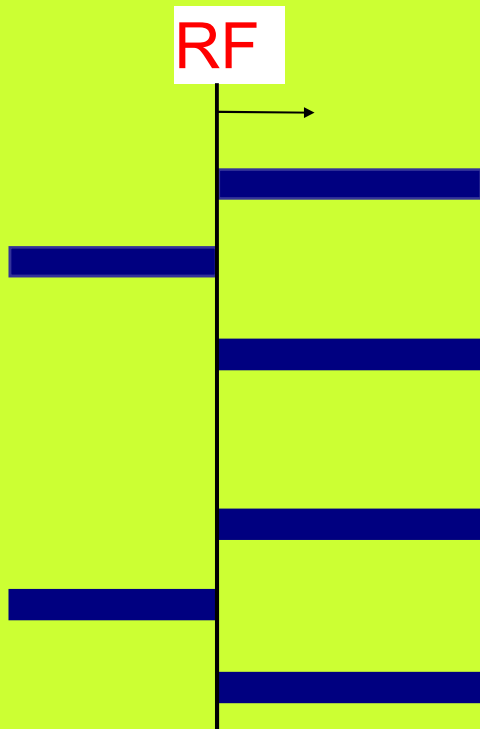


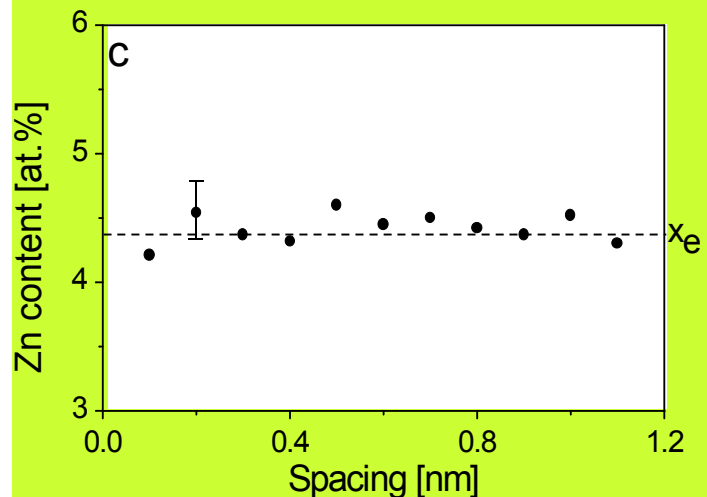
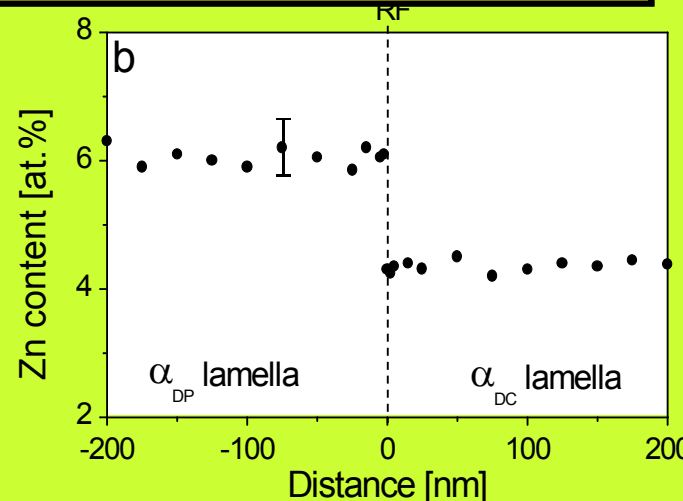
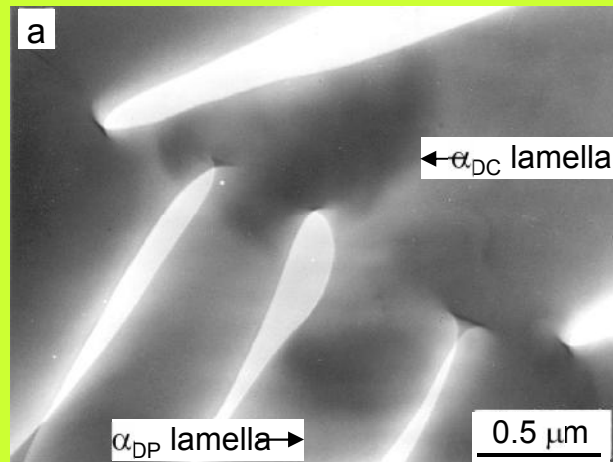
Discontinuous coarsening



Ni-10 at.% Sn aged at 924 K for 4 h,
M.Frebel, B. Predel, M.Klisa,
Z. Metallkunde 65 (1974) 469

$(\alpha+\beta)_{\text{fine}} \rightarrow (\alpha+\beta)_{\text{coarse}}$

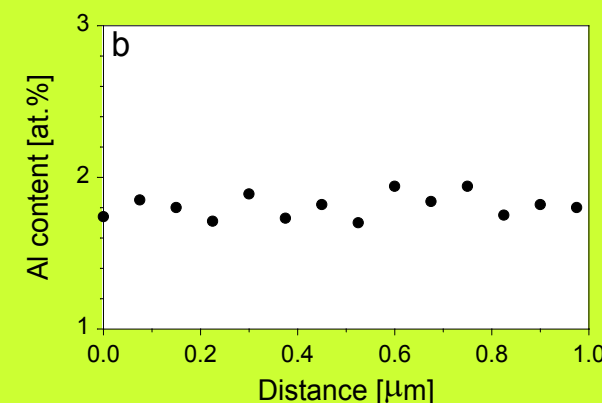
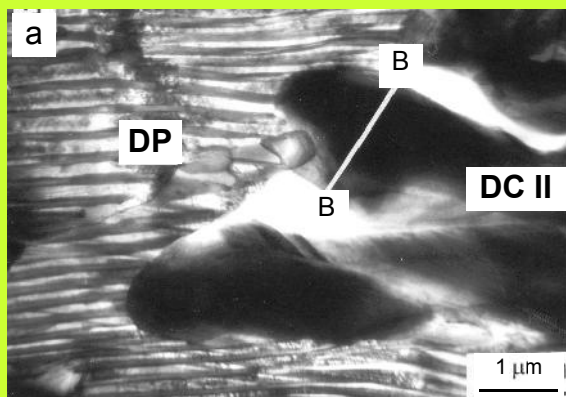
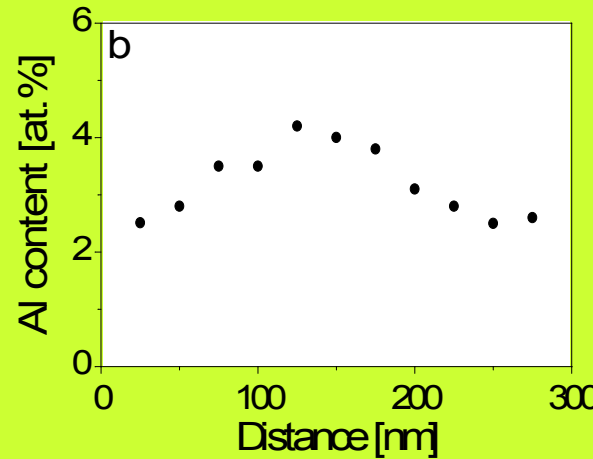
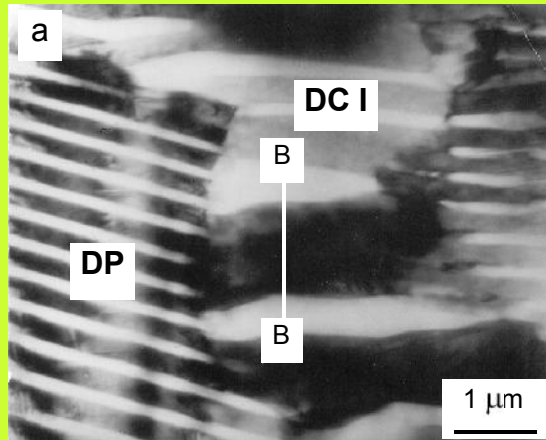
Discontinuous coarsening



- Thickness of the α lamella several times larger than for DP,
- Abrupt concentration change across RF (α_{DP}/α_{DC} interface),
- Usually flat solute concentration profile across the α_{DC} lamellae corresponding to equilibrium concentration, x_e .
- Possibility of further DC reactions (DC II, DC III).

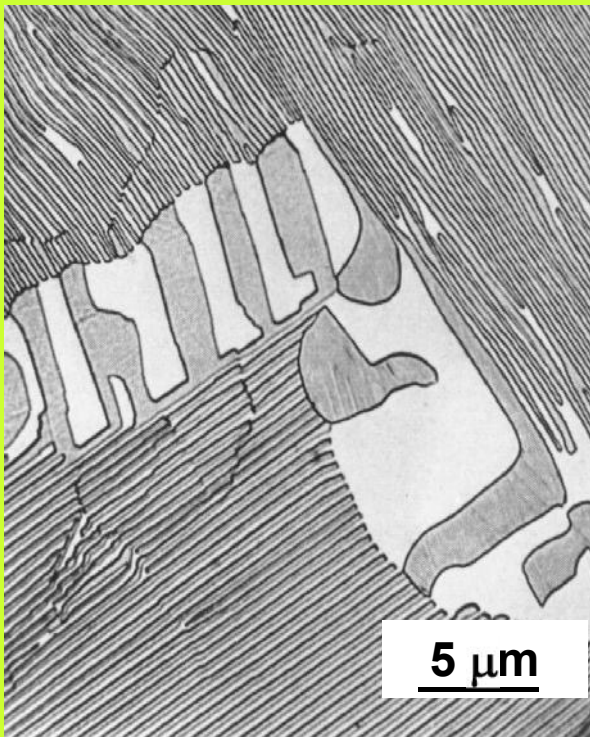
Al-22 at.% Zn aged at 450 K for 350 h

Discontinuous coarsening

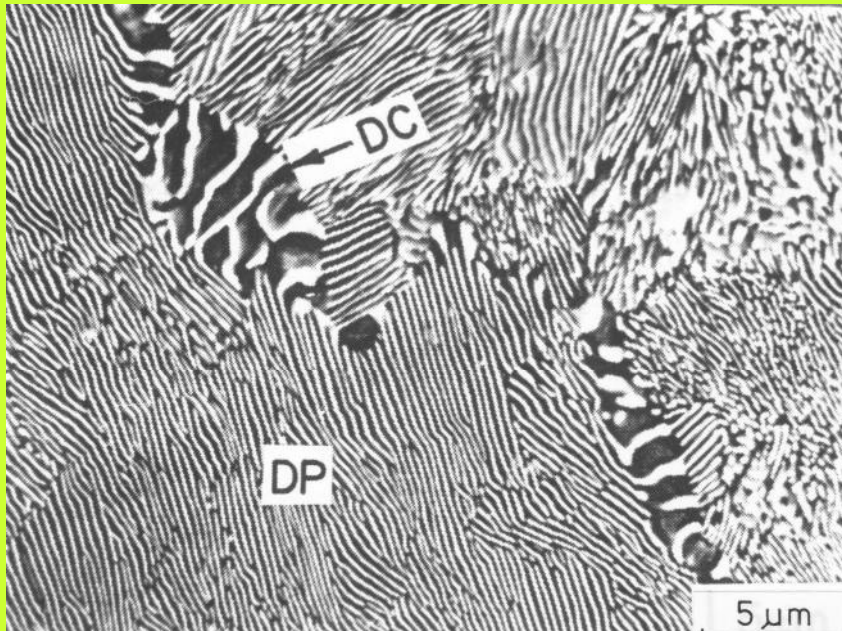


P. Zięba:
Acta Mater. 46 (1998) 369
Co-13 at.% Al
aged for 20 days at 850 K.

Discontinuous coarsening

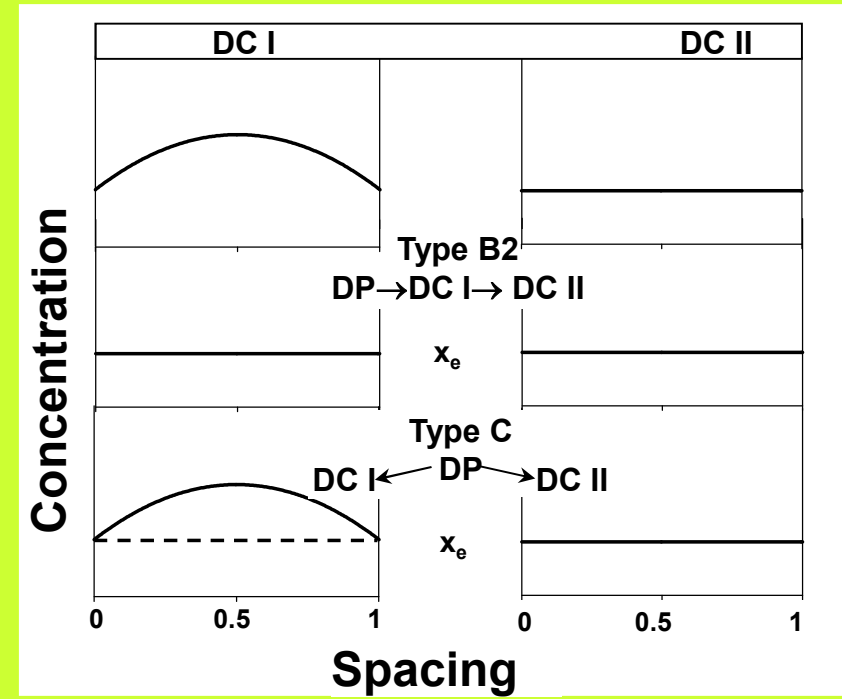
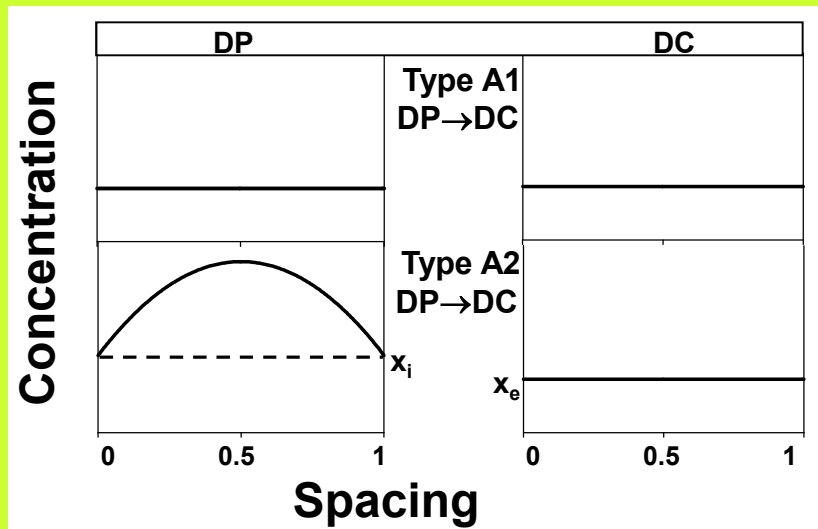


J.D. Livingston, J.W. Cahn:
Acta metall. 22 (1974) 495
Co-Si alloy aged 4 days at 373 K

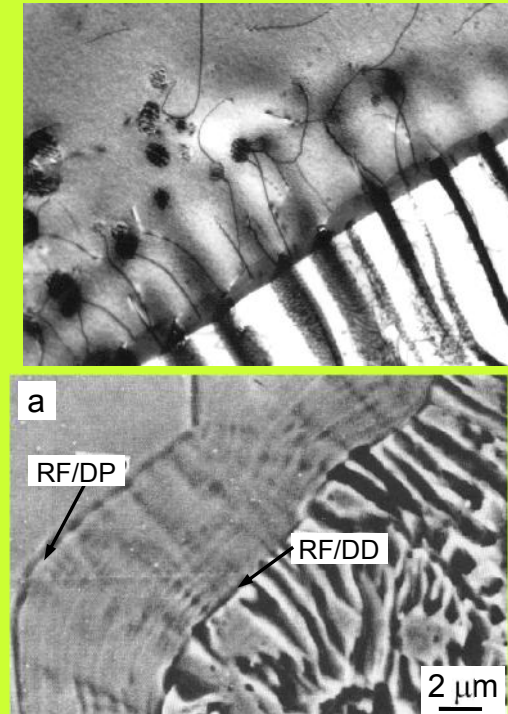
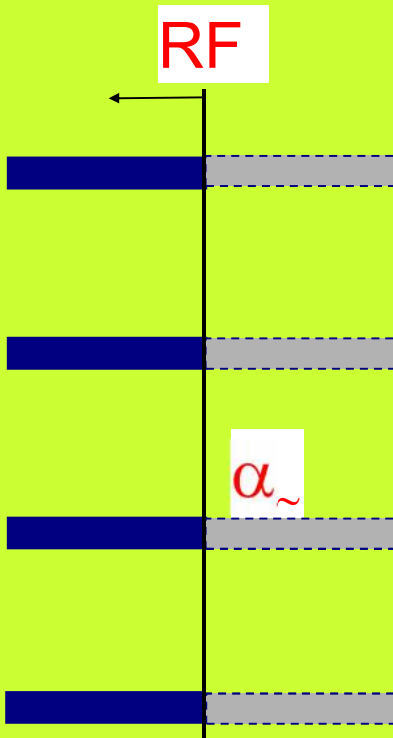


Y.Yang, G. Sarkar, R.A. Fournelle:
Acta metall. 27 (1979) 1147
Al-39.3 at.% Zn aged at 523 K for 1 h

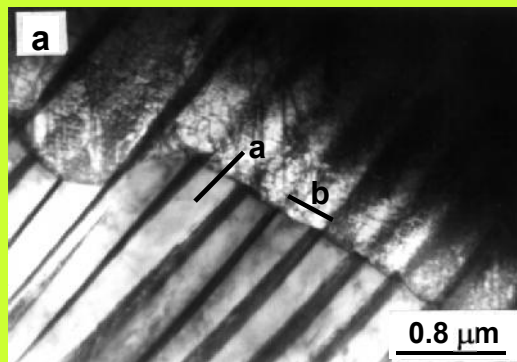
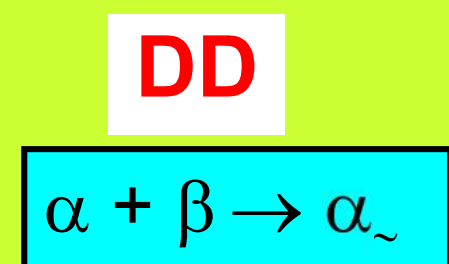
Discontinuous coarsening



Discontinuous dissolution-principle



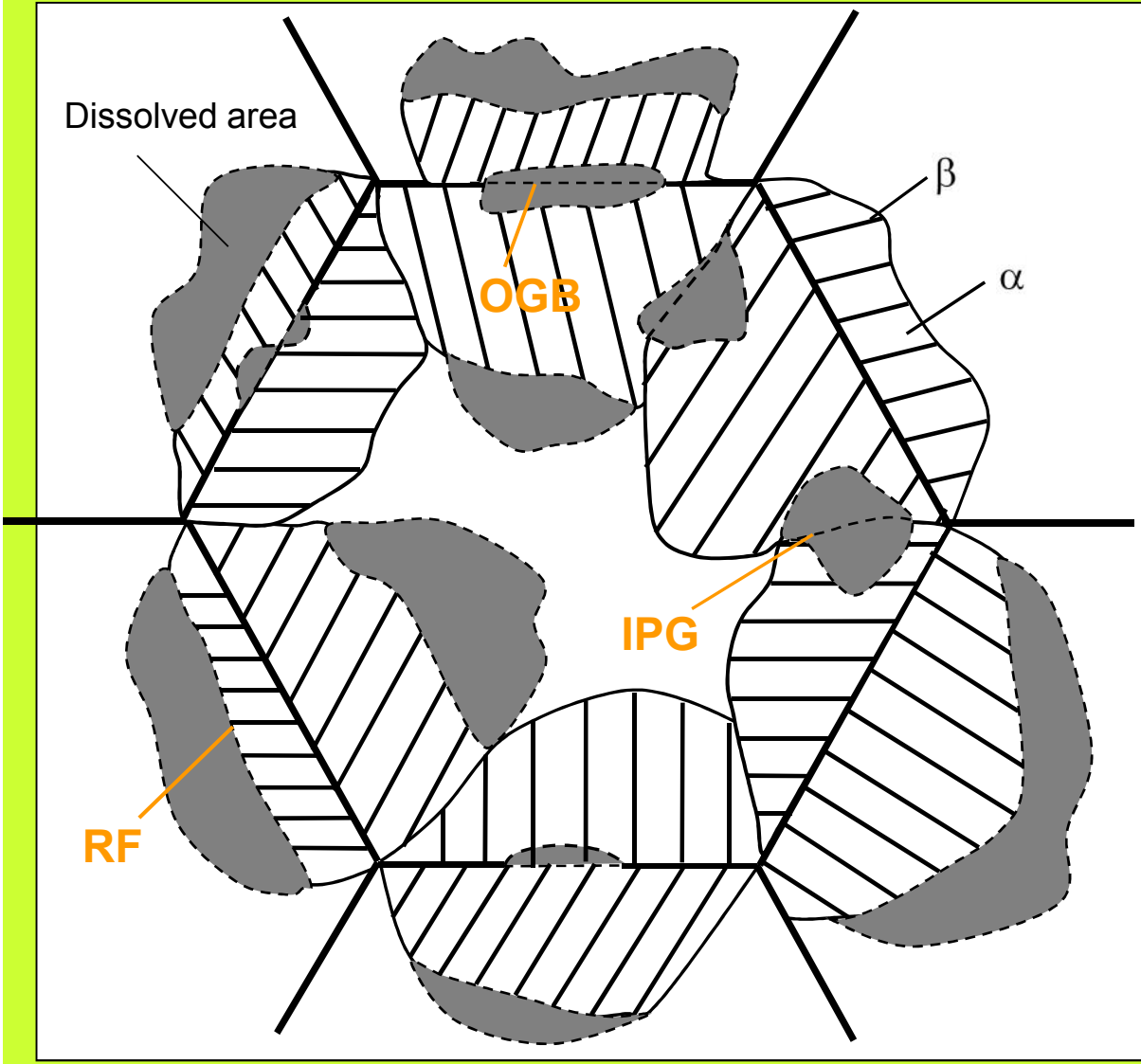
Al-22 at.% Zn aged at 448 K for 540 s. Dissolution at 603 K for 1 s
P. Zięba:
PhD dissertation, IMIM PAN 1987



Fe-13.5 at.% Zn aged at 723 K,
Dissolution 886 K
T.H. Chuang, R.A. Fournelle, W.
Gust, B. Predel:
Z. Metallkde 80 (1989) 175

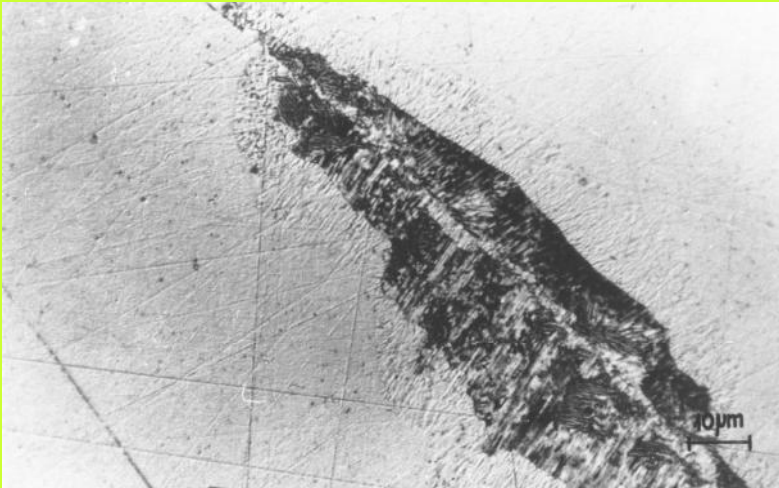
Ni-4 at.% Sn starzony 200 h w 725 K, a następnie przez 60 h w 775 K. Rozpuszczanie przez 30 s w 945 K
P. Zięba, W. Gust:
Acta Mater. 47 (1999) 2641

DD-initiation sites

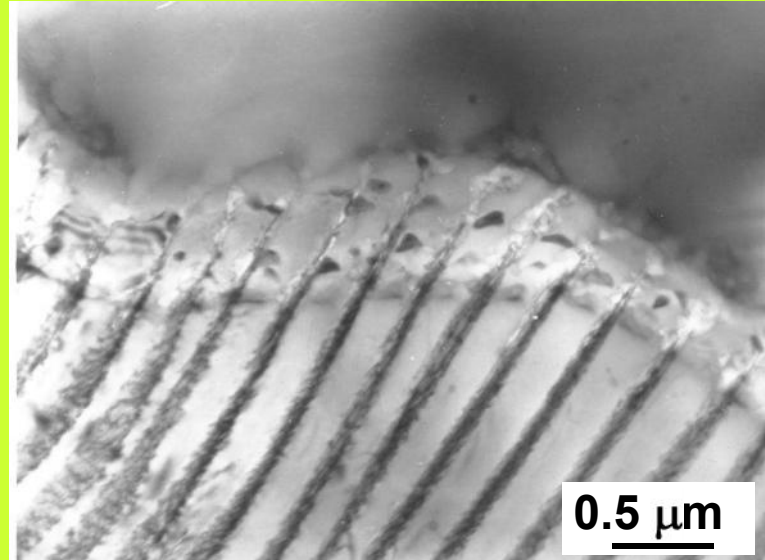


- ❖ Primary grain boundary (OGB)
- ❖ Reaction front of DP (RF)
- ❖ Impingement of two colonies of discontinuous precipitates (IPG)

DD-morphology

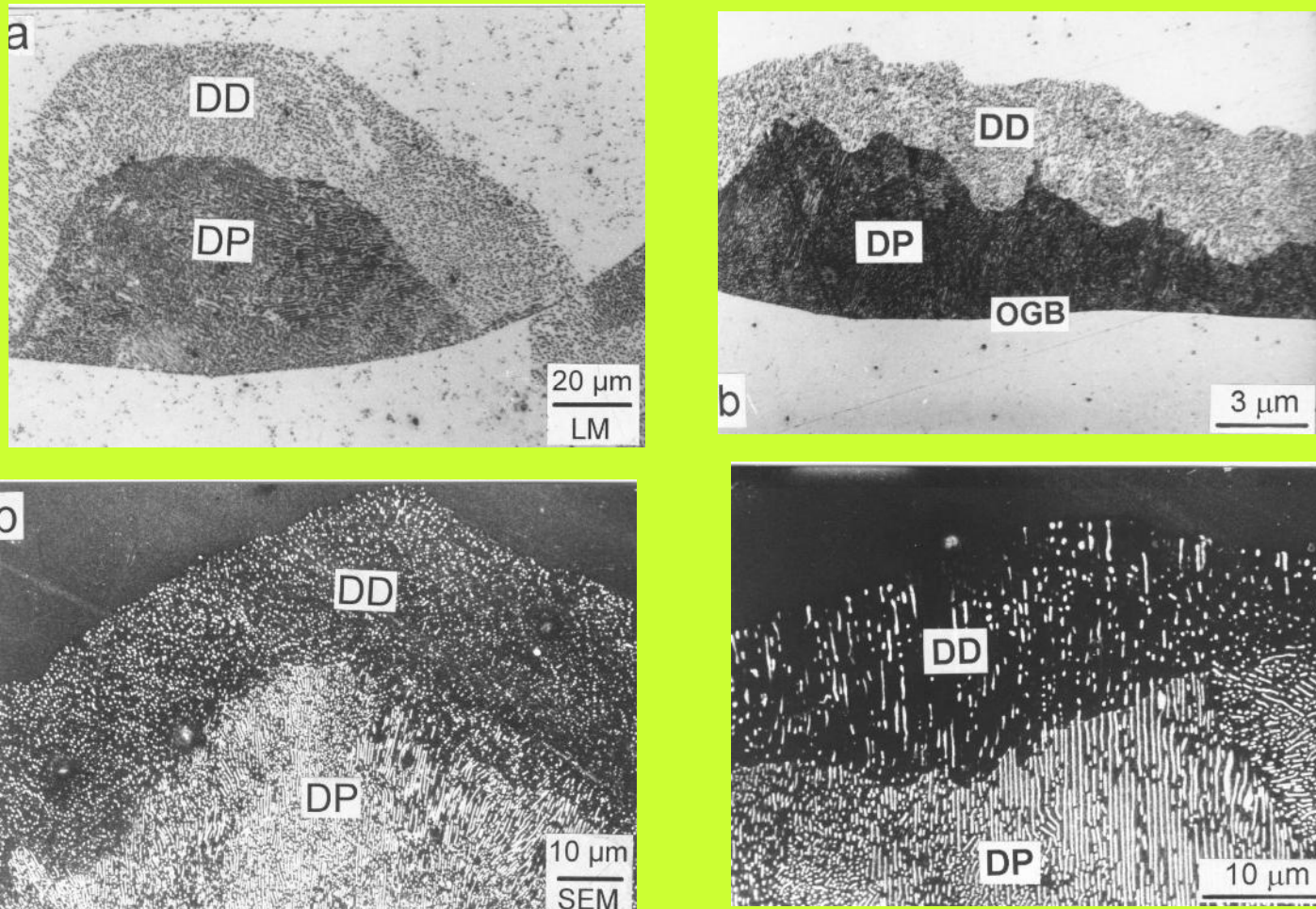


Ni-4 at.% Sn aged at 775 K for 200 h.
Dissolution at 945 K for 15 min



Al-22 at.% Zn aged at 450 K for 10
min. Dissolution at 560 K for 5 s

DD-morphology



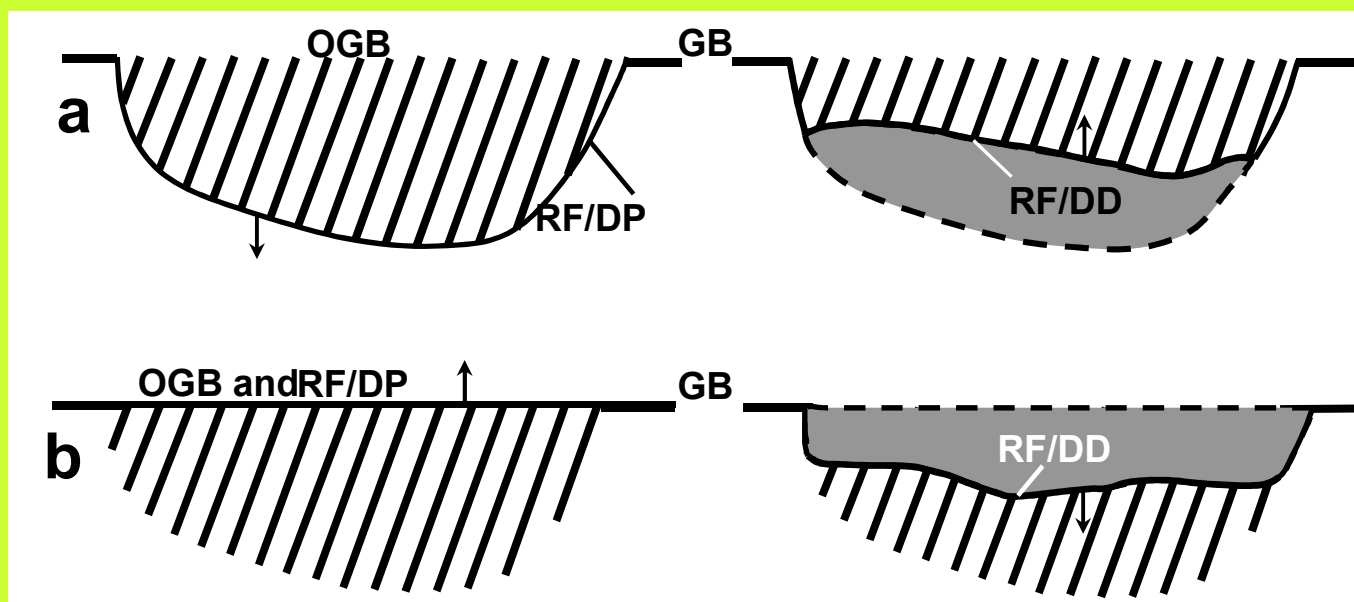
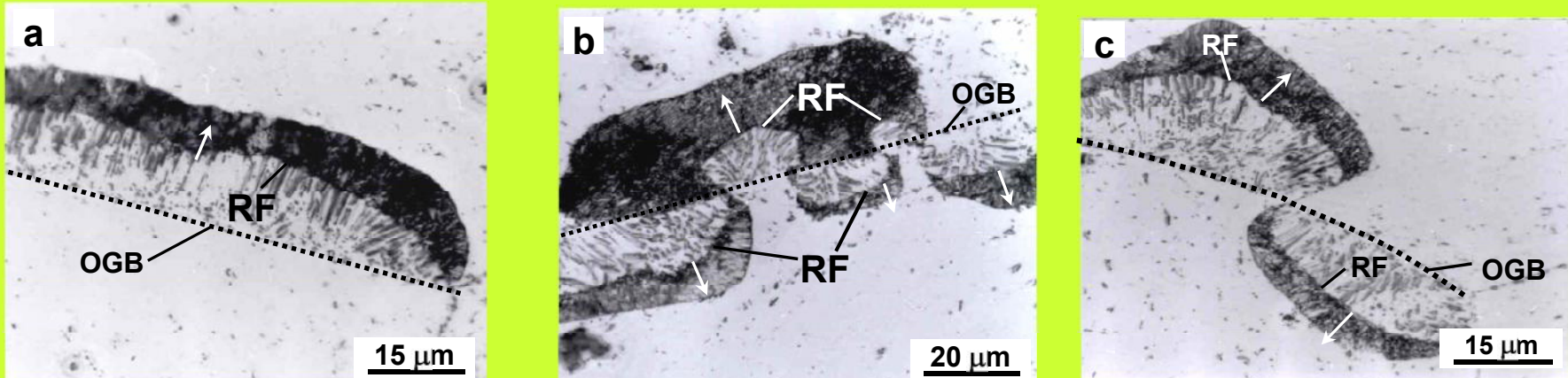
D. Bradai, P. Zięba, W. Gust, M. Hadi Kanifi: *Practical Metallography* 35, (1998) 673

D. Bradai, M. Kadi Hanifi, P. Zięba, W.M. Kuschke, W. Gust: *Journal of Materials Science* 34, (1999) 5331

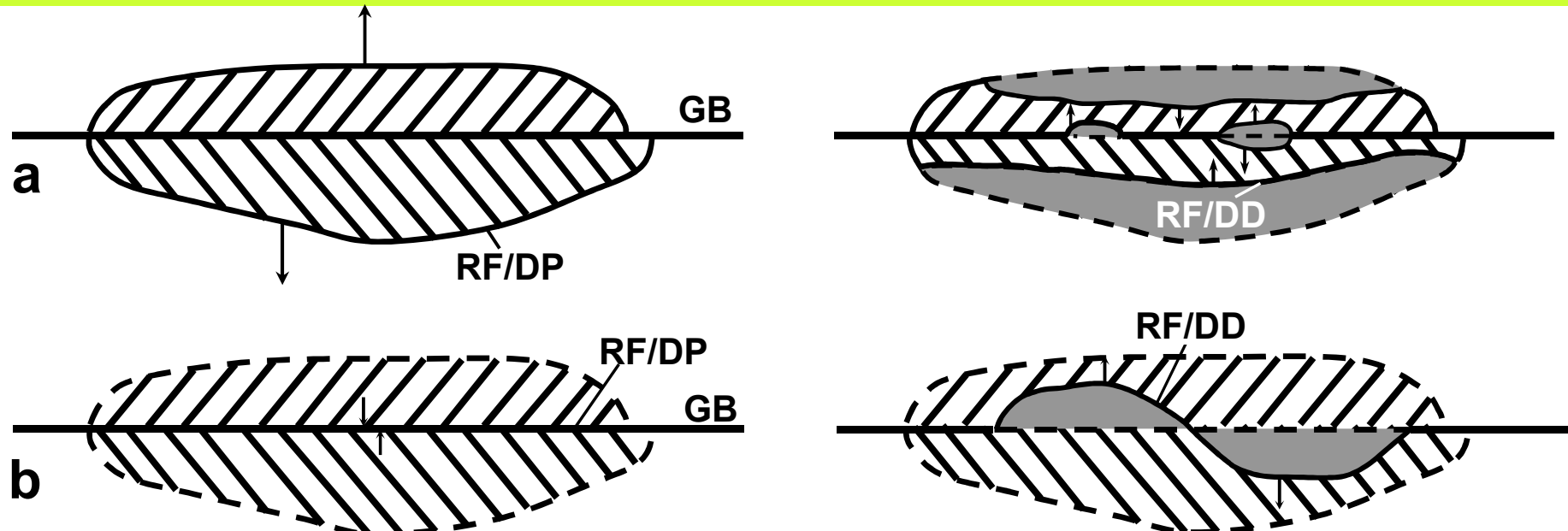
DD- morphology

Mg-10 wt.% Al aged at 495 K for 30 min, then annealed at 695 K for 30 min (times). Subsequent ageing at 495 K for 30 min and annealed at 645 K for 7 min.

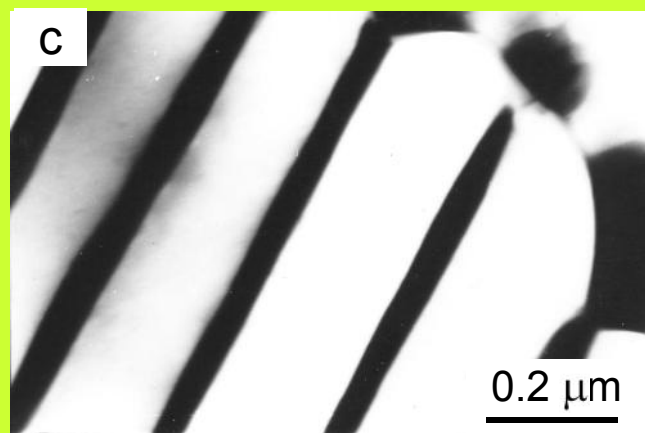
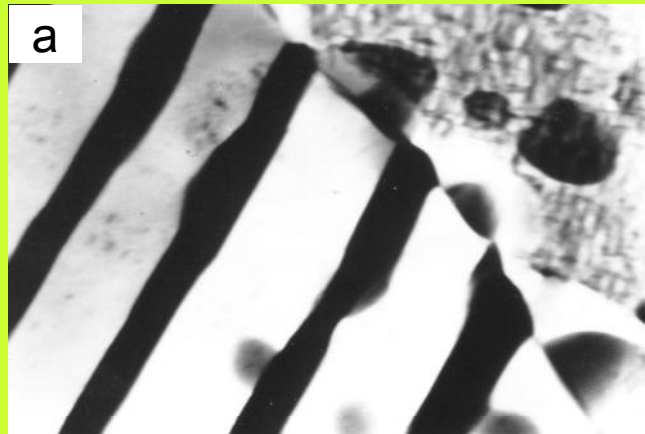
D. Bradai, P. Zięba, E. Bischoff, W. Gust: *Materials Chemistry and Physics* 72 (2001) 401



DD-morphology



DD-in situ studies

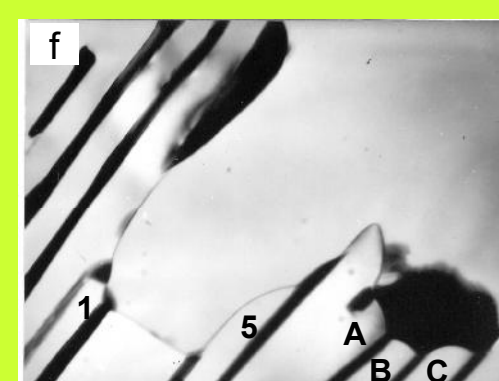
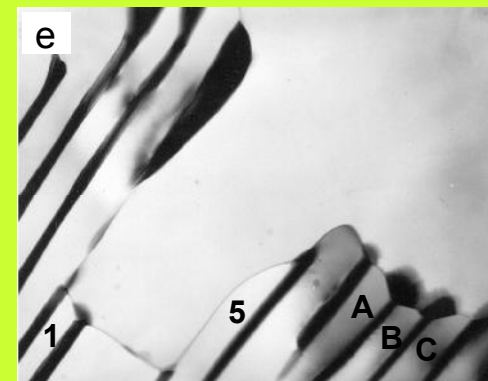
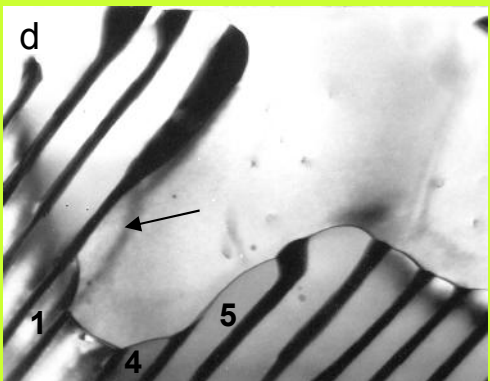
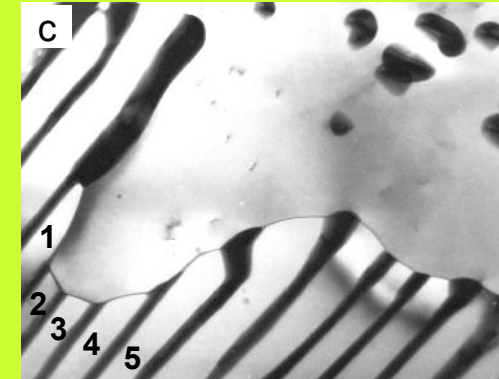
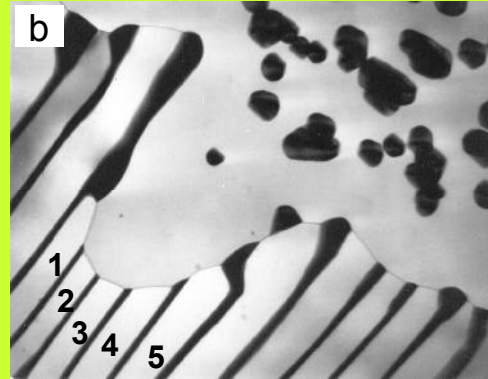
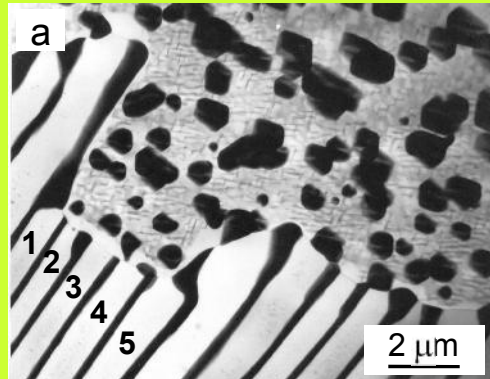


P. Zięba, J. Morgiel: *Scripta Metall. Mater.* 30 (1994) 1177

P. Zięba: *Z. Metallkunde* 90 (1999) 9

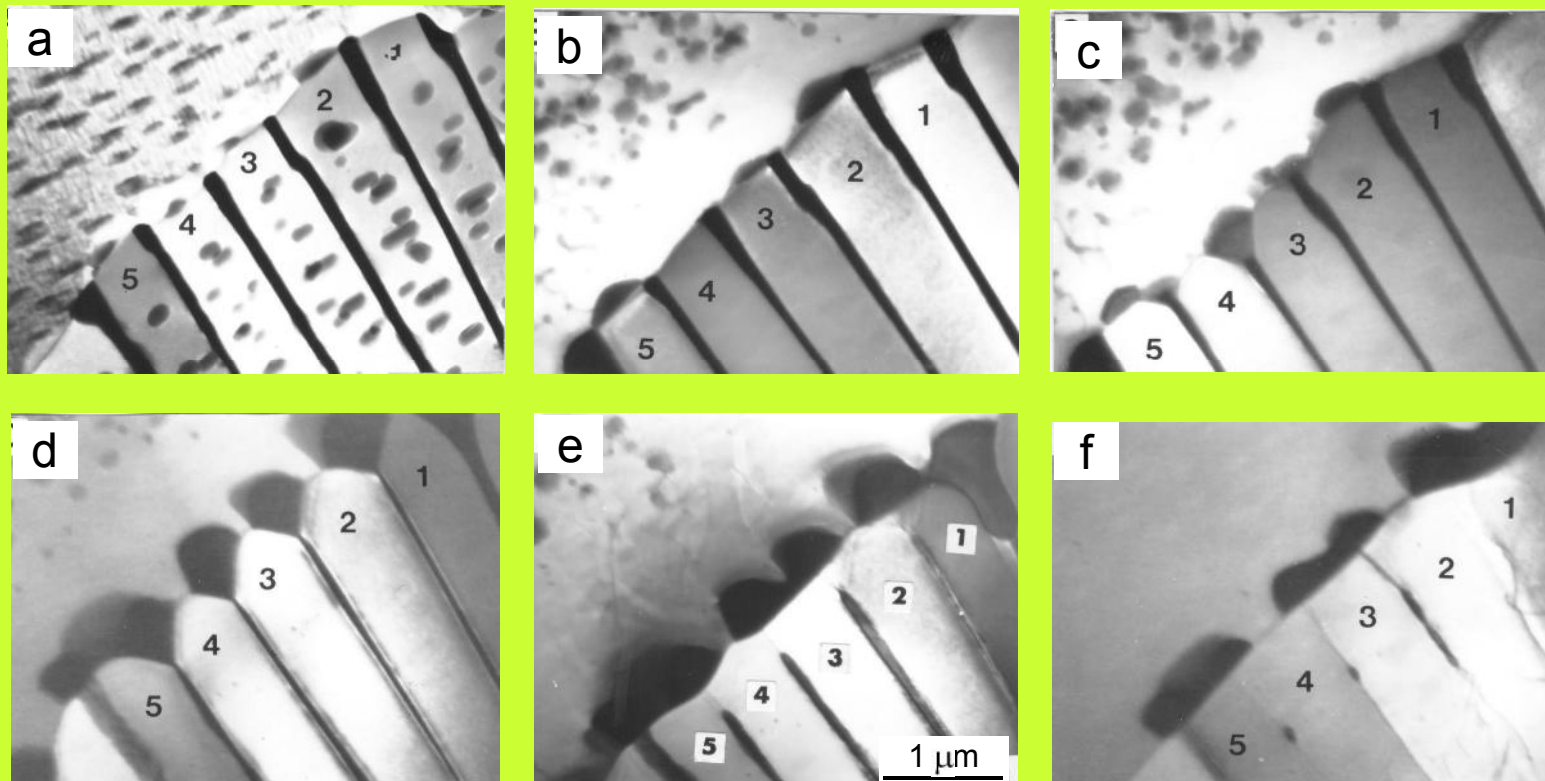
Al-22 at.% Zn aged at 440 K for 20 min. Dissolution at 575 K for 10 sec

DD-in situ studies



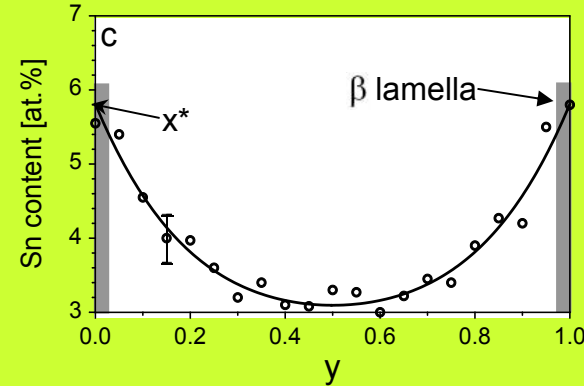
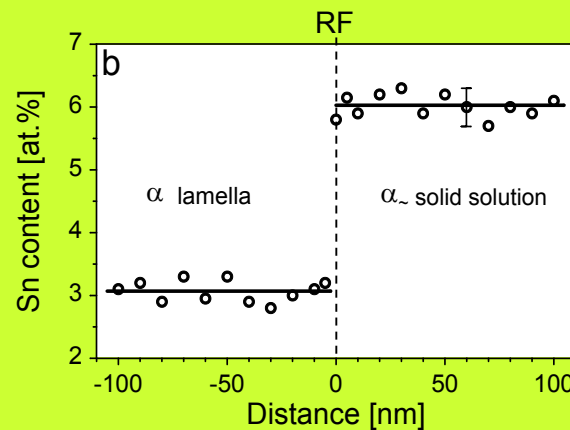
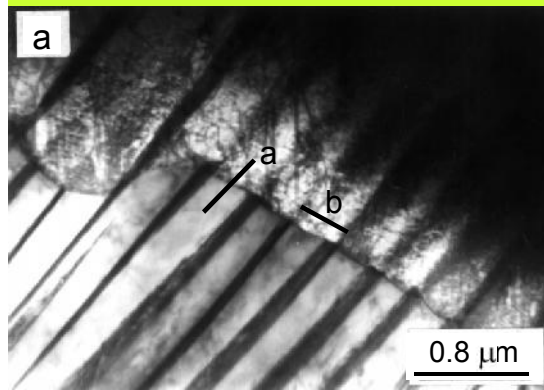
P. Zięba: Z. Metallkunde 90 (1999) 9
Al-22 at.% Zn aged at 450 K for 10 min. Dissolution at 550 K for 30 s

DD-in situ studies



P. Zięba, A. Pawłowski: *Mater. Sci. Eng.* A187 (1994) 57
Al-22 at.% Zn aged at 450 K for 10 min. Dissolution at 570 K for 20 s

DD-solute concentration profiles

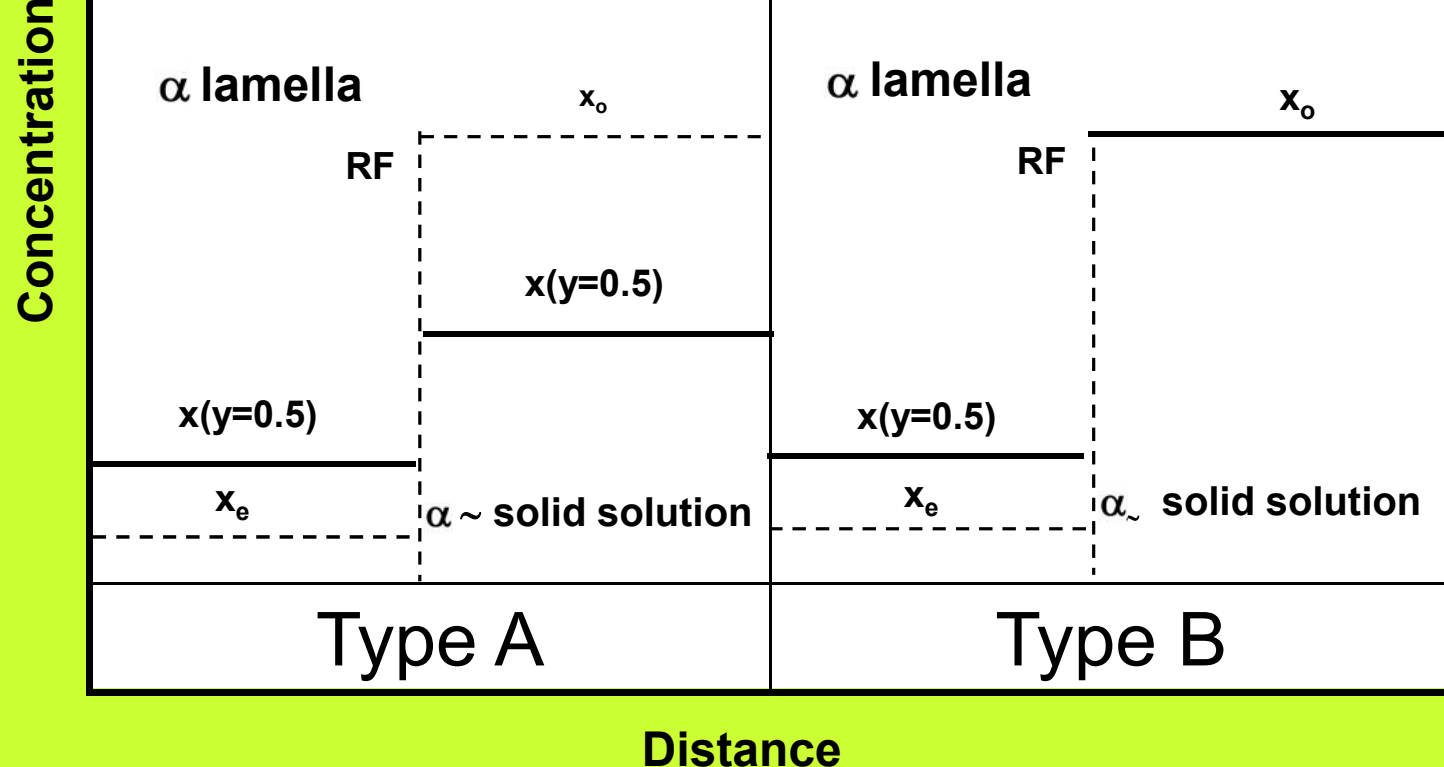


Ni-4 at.% Sn aged 200 h at 725 K, and then 60 h at 775 K. Dissolution for 30 s at 945 K
P. Zieba, W. Gust: *Acta mater.* 47 (1999) 2641

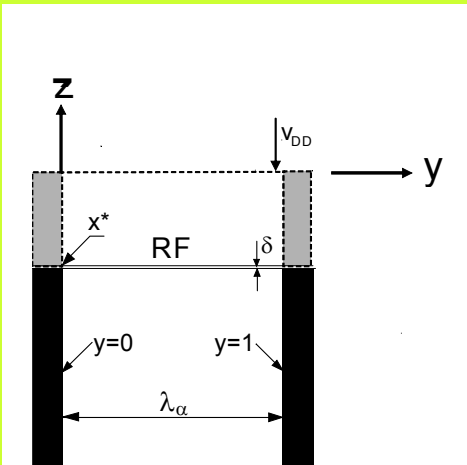
- “Ghost images” showing inhomogeneity of solute concentration in α_{\sim} solid solution formed due to dissolution,
- Abrupt change of solute content across the reaction front (line a),
- „U” shape of solute concentration profile in α_{\sim} solid solution measured along line b,
- The highest value of solute content (denoted as x^*) corresponding to the place just behind the dissolved tip of the β phase,
- „Depth” of solute concentration profile much more pronounced than „height” during DP reaction.

DISCONTINUOUS DISSOLUTION

Solute concentration profile across RF



DD- model



T-T equation

K.N.Tu, D.B. Turnbull

Metall. Trans. A2 (1971) 2509

Assumption: $p=z$, A constant incorrectly calculated

Z-P equation

P. Zięba, A. Pawłowski: *Scripta Metall.* 20 (1986) 1653

$$x'(y) = A \sinh(zy\lambda_\alpha) + B \cosh(zy\lambda_\alpha) + \frac{a}{p^2 - z^2} \cosh(py\lambda_\alpha) - \frac{b}{p^2 - z^2} \sinh(py\lambda_\alpha) + x_o$$

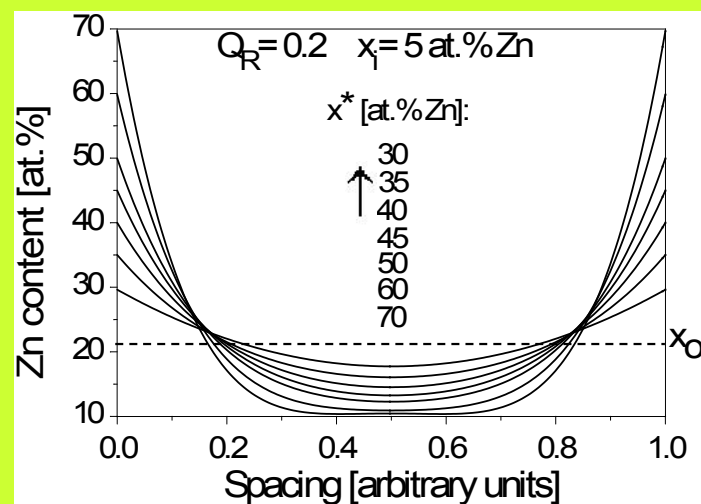
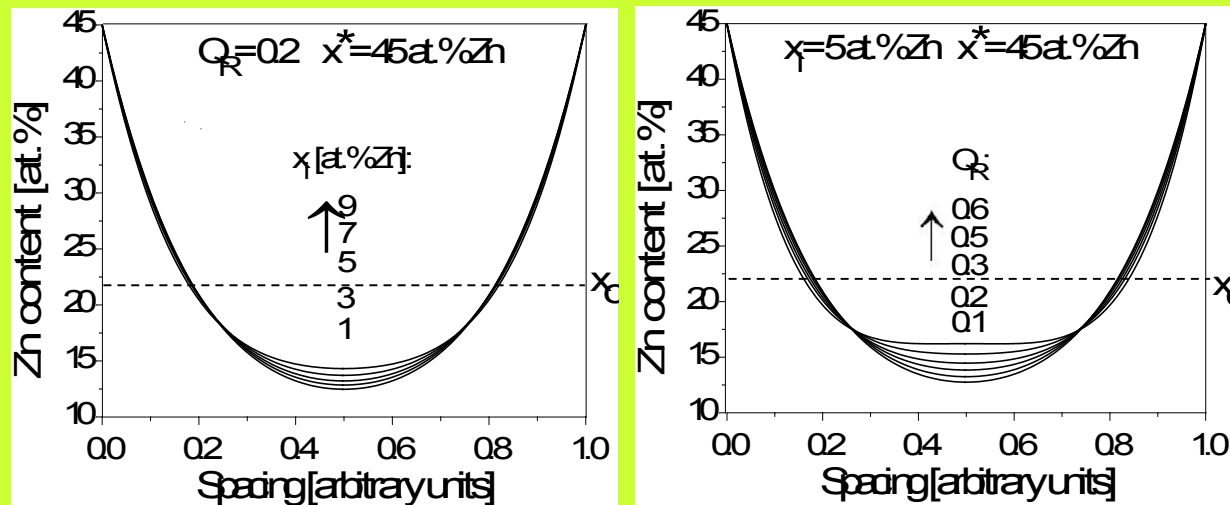
$$p = \left(\frac{v_{DP}}{s \delta D_b} \right)^{\frac{1}{2}}, z = \left(\frac{v_{DD}}{s \delta D_b} \right)^{\frac{1}{2}}$$

$$\mathbf{A}, \mathbf{B}, \mathbf{a}, \mathbf{b} = \mathbf{f}(x_o, x_e, x^*, \lambda_\alpha, z, p)$$

Considering atoms flux at the tip of β phase lamella

$$\lambda_\beta x_\beta = \frac{2}{z} \left[\left(x^* - x_o - \frac{z^2(x_o - x_i)}{p^2 - z^2} \right) \tanh(z\lambda_\alpha / 2) + \frac{pz(x_o - x_i) \tanh(p\lambda_\alpha / 2)}{p^2 - z^2} \right].$$

DD-simulation



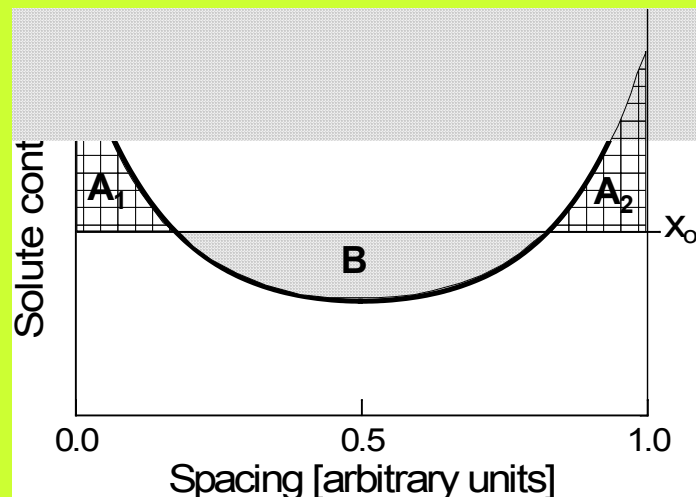
$$Q_R(y) = \frac{x(y) - x_i}{x_o - x_i} = 1 - \frac{\cosh[(y - 0.5)p\lambda_\alpha]}{\cosh(p\lambda_\alpha / 2)}$$

P. Zięba, W. Gust
Interface Science 6 (1998) 309

DD- validity of Z-P equation

P. Zięba, W. Gust: *Interface Science* 6 (1998) 309

Only those concentration profiles are admissible for which the areas above and under the level of the concentration x_o fulfill the relation $A_1+A_2=B$



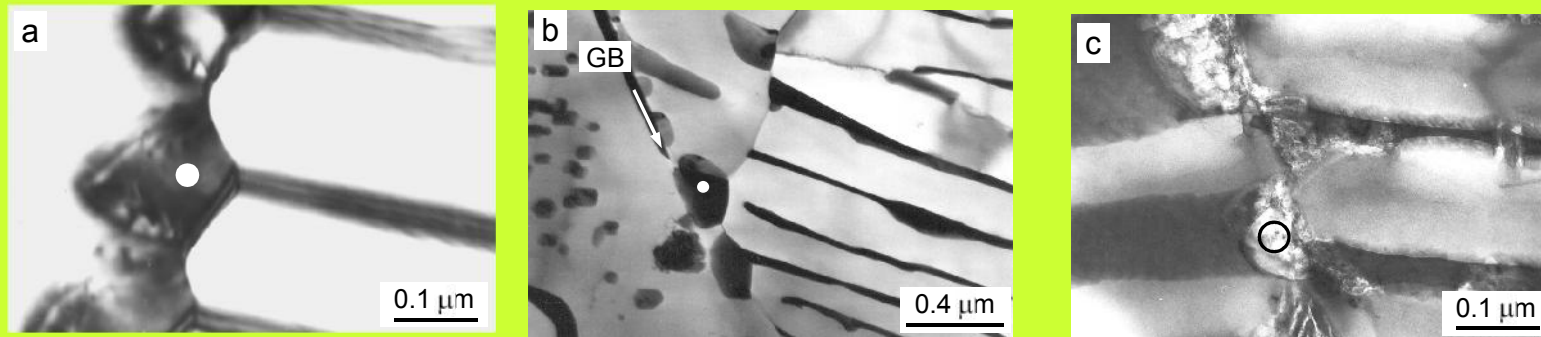
$$\int_0^1 (x'(y) - x_1) dy = 0$$

$$x_1 = x_o + \frac{2}{\lambda_\alpha} \left[\frac{B}{z} \tanh \left(\frac{z \lambda_\alpha}{2} \right) + \frac{a \tanh (p \lambda_\alpha / 2)}{p (p^2 - z^2)} \right].$$

If $x_1 = x_o$, then

$$x^* = x_o + \frac{a}{p^2 - z^2} \left[1 - \frac{z \tanh (p \lambda_\alpha / 2)}{p \tanh (z \lambda_\alpha / 2)} \right]$$

DD – x^* concentration



RF

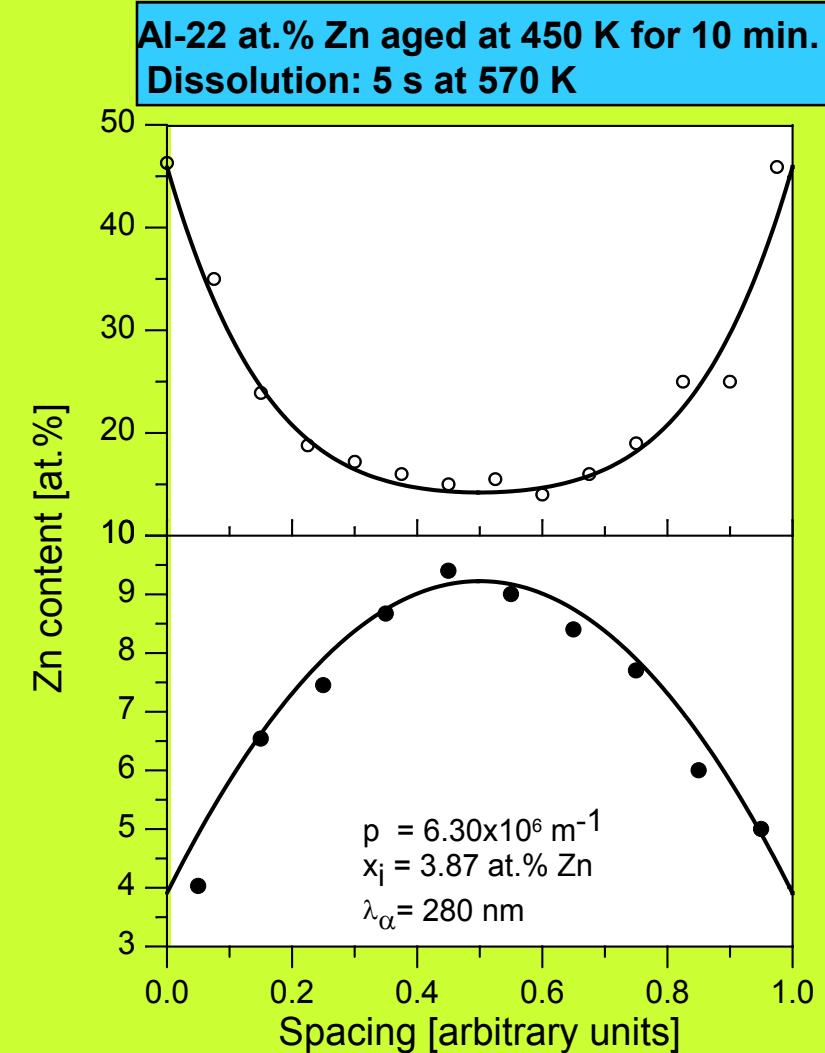
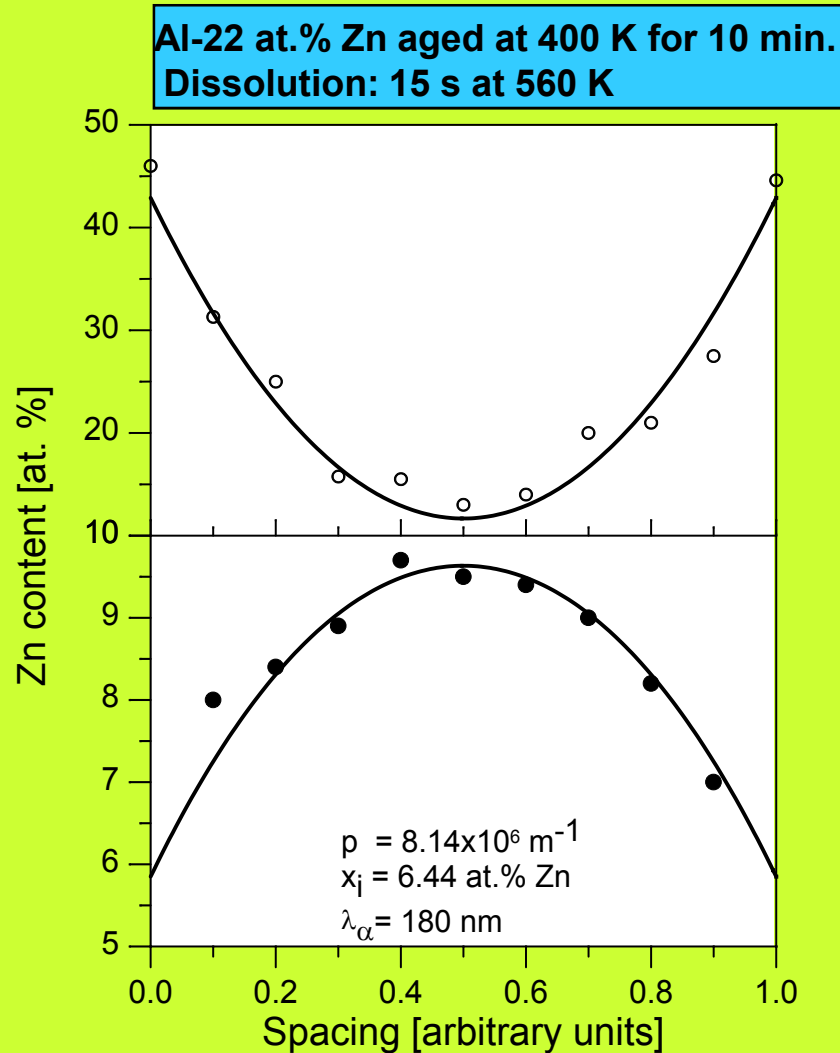
OGB

IPG

P. Zięba, W. Gust: *Inter. Mater. Rev.* 43 (1998) 70
Al-22 at.% Zn aged at 450 K for 3 min

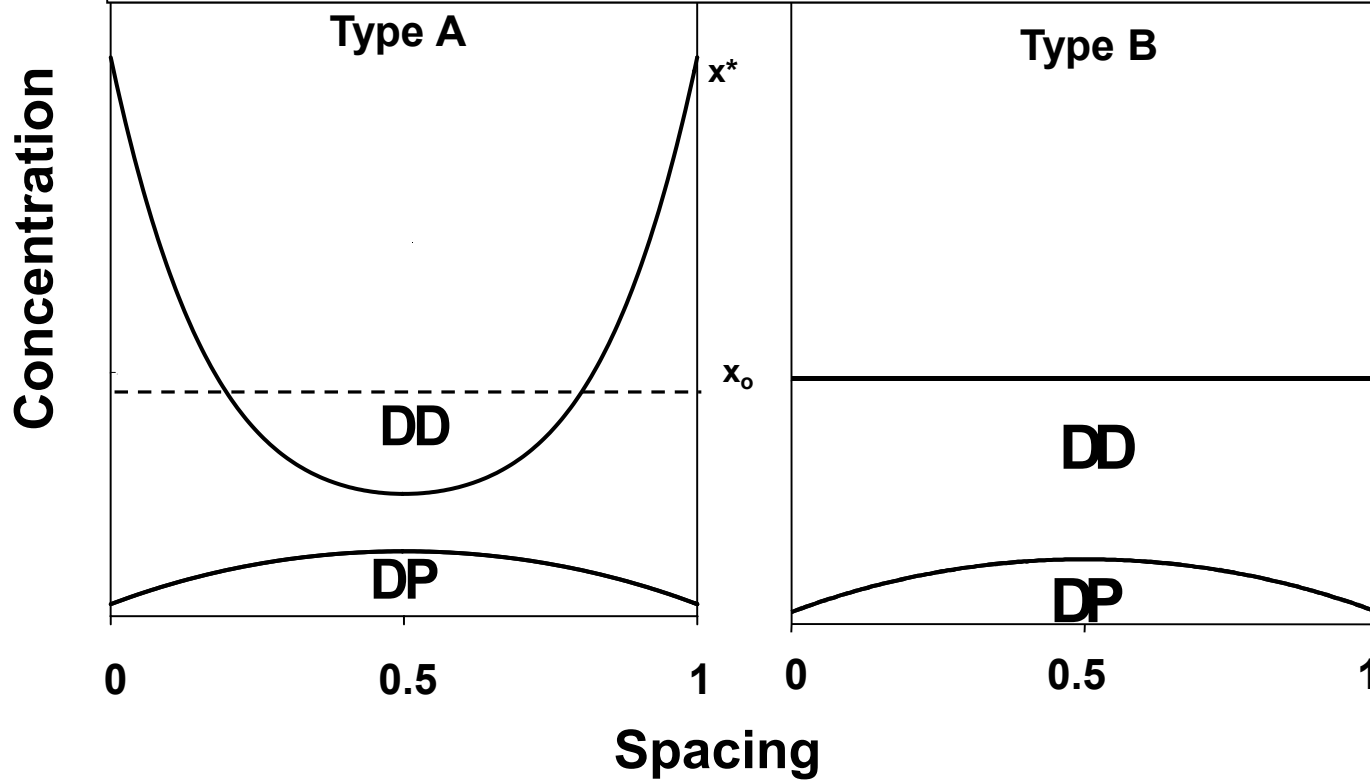
Temperature [K]		Concentration, x^* [at.-%]		
DD	DP	RF	OGB	IPG
560		46	45.2	47
570	450	45	44.6	45.2
580		43.5	43.1	43.3
590		43	42.8	43

DD-solute concentration profiles

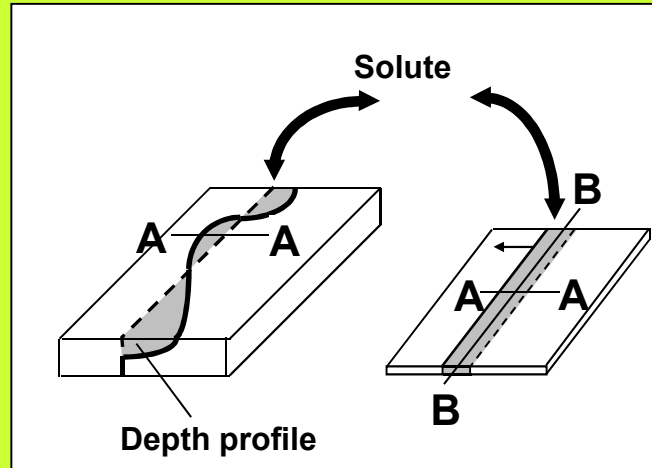


DISCONTINUOUS DISSOLUTION

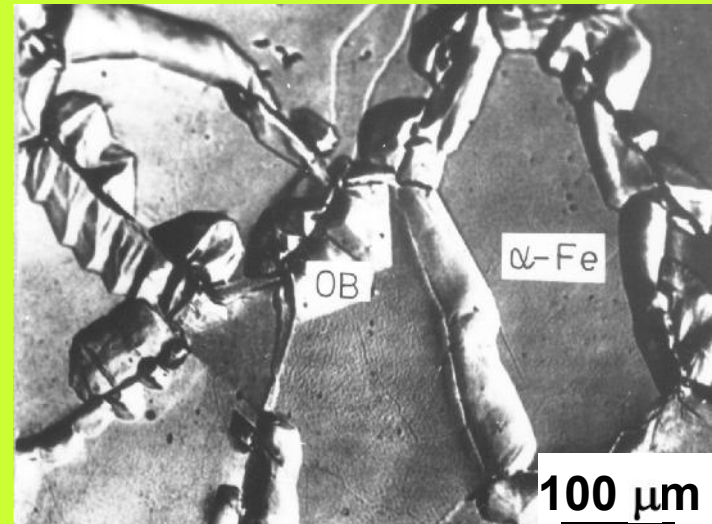
Solute concentration profile parallel to the RF



DIFFUSION INDUCED GRAIN BOUNDARY MIGRATION



M. Hillert, G.R. Purdy,
Acta metall. 26 (1978) 333

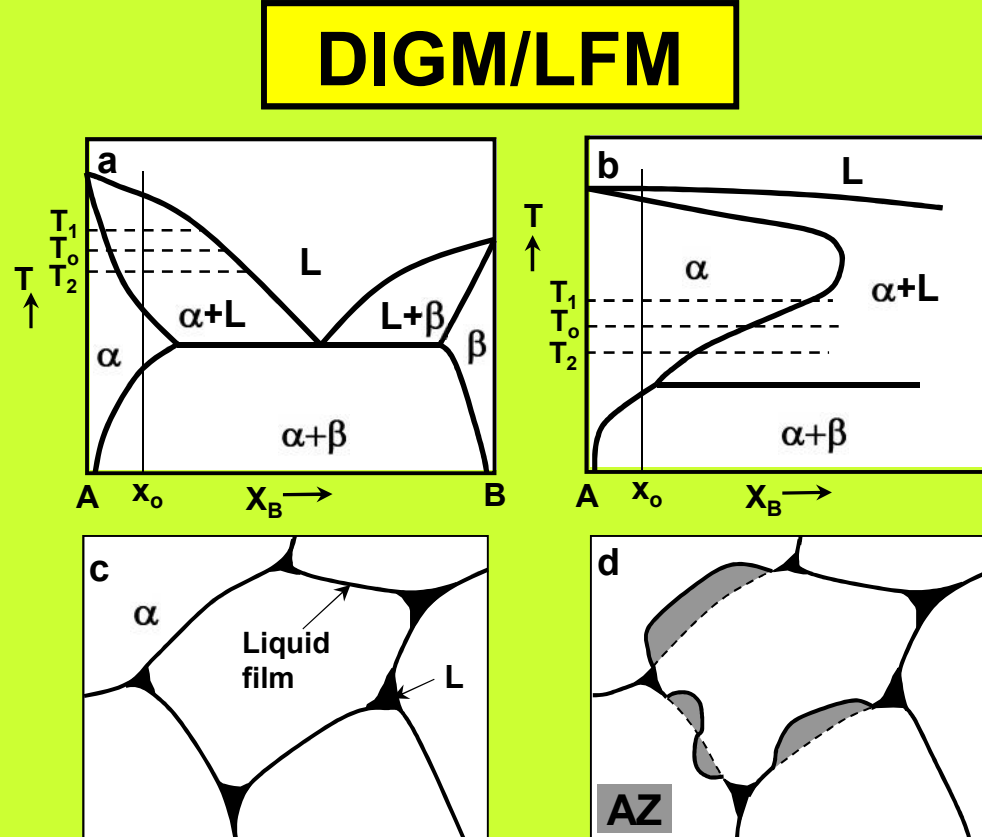


DIGM – Diffusion induced grain boundary migration

Phenomenon associated with the migration of a grain boundary into a pure metal or solid solution caused by the diffusion of solute atoms into or out of the material along the boundary. In a consequence, the region behind the moving boundary is enriched or depleted with solute atoms, which is manifested by an alloyed or de-alloyed zone, respectively.

CIGM – Chemical induced grain boundary migration

Encounters also the cases where the chemical instability leading to the grain boundary migration is induced by a temperature or atmosphere change for the internal solute sink or source.

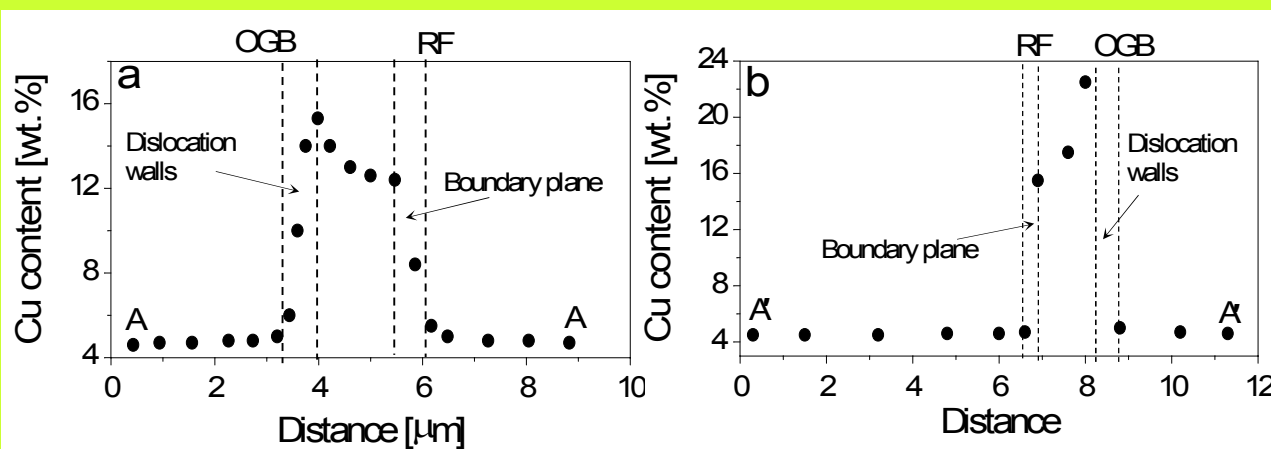
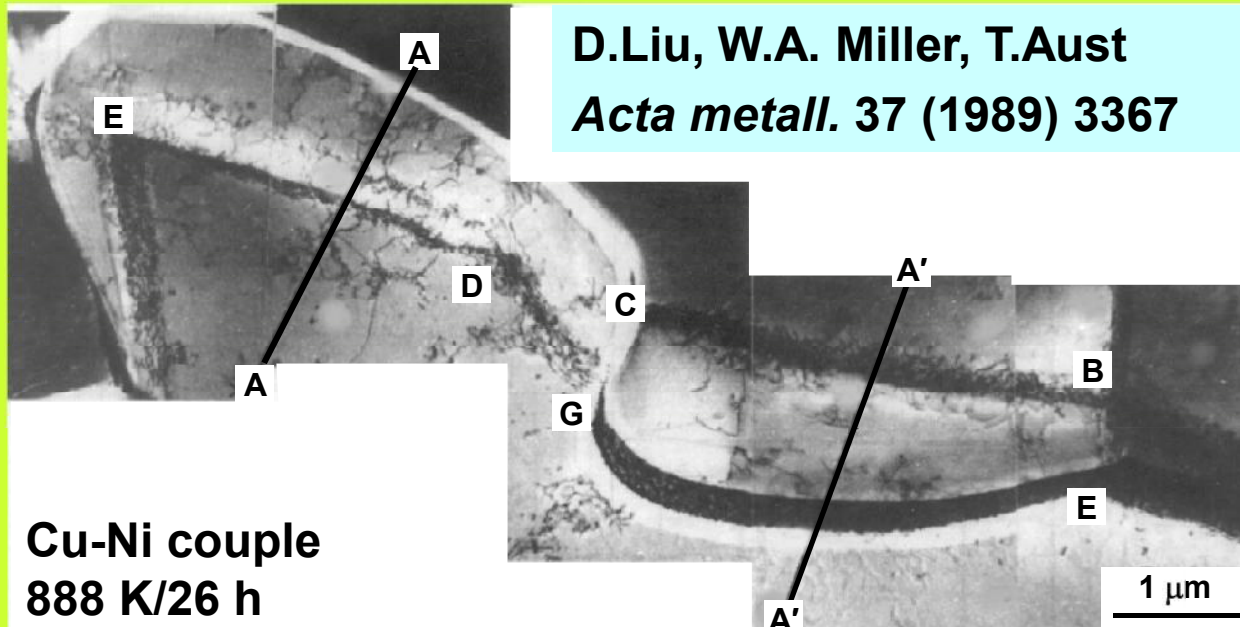


LFM – Liquid film migration

found in partially molten samples either when liquid is first introduced or when the chemical composition of the liquid is changed, for example, by alloying or by changing the temperature.

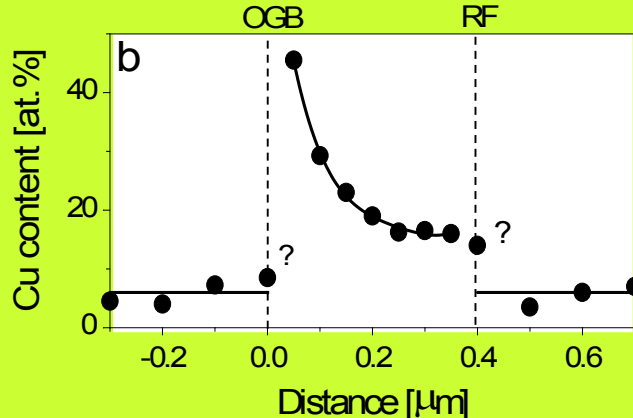
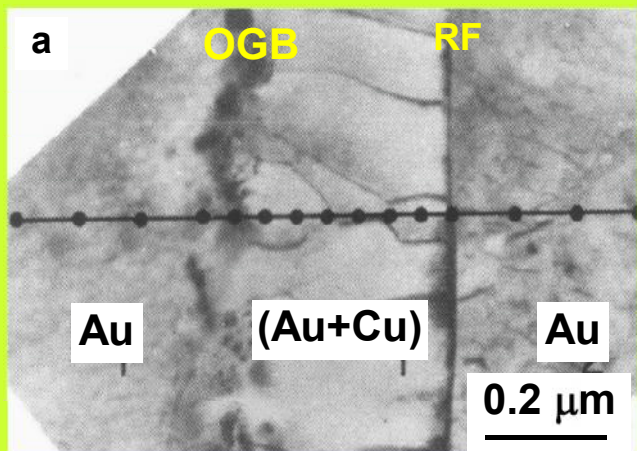
DIGM

Solute profile across RF

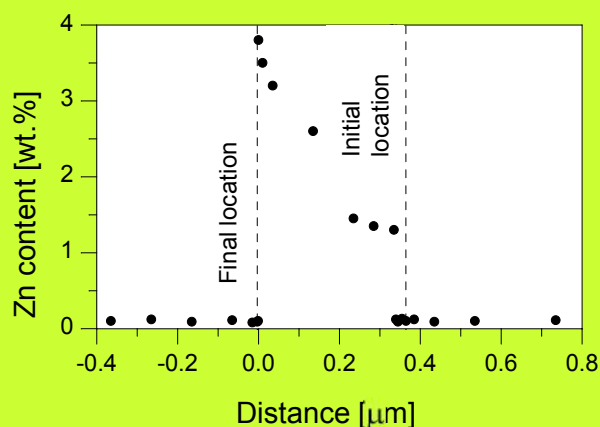
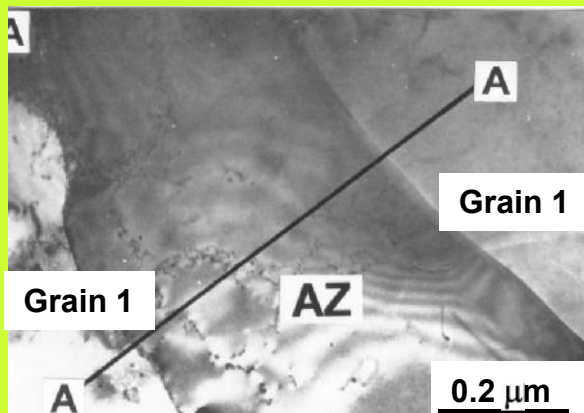


DIGM

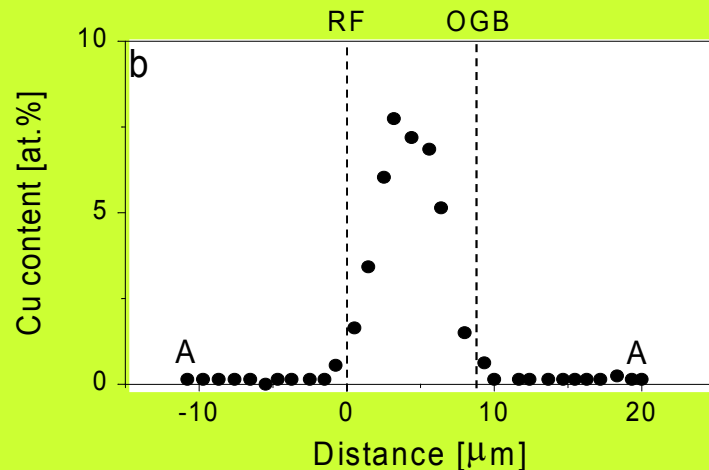
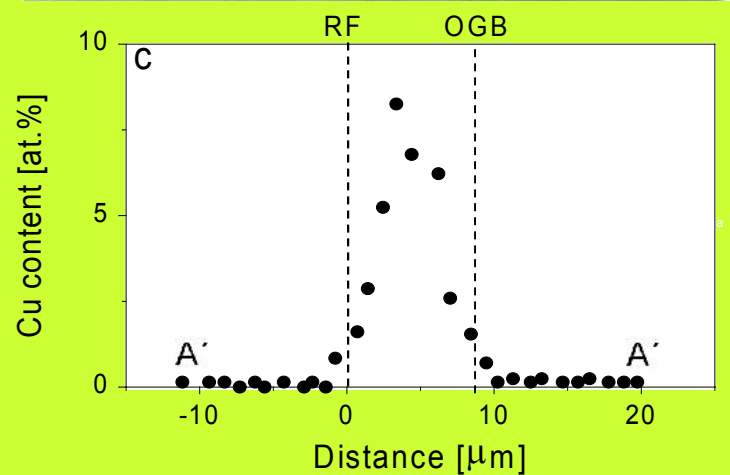
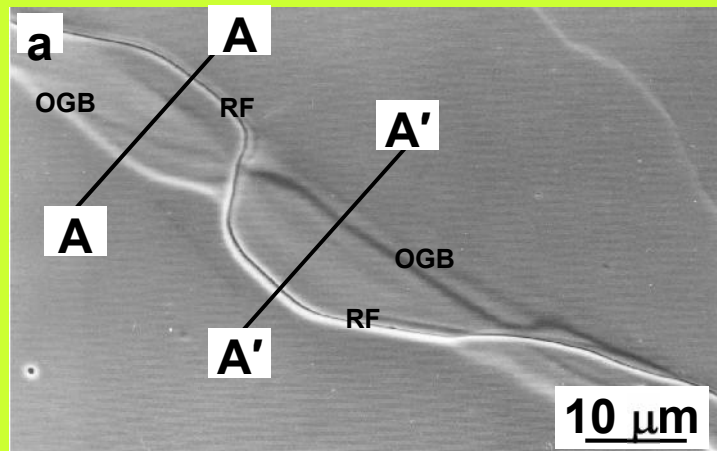
Solute profile across RF



J.W. Pan, R.W. Baluffi:
Acta metall. 30 (1982) 861
Cu-Au couple: 423 K/137 h



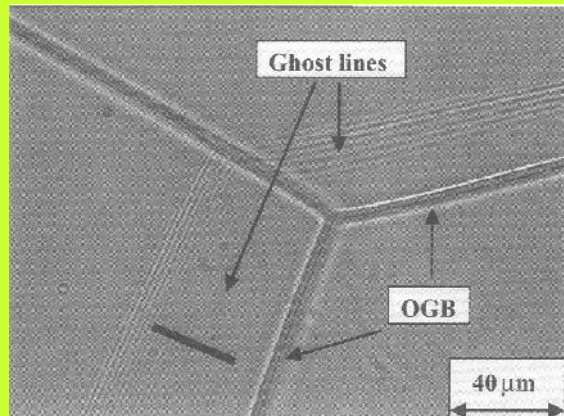
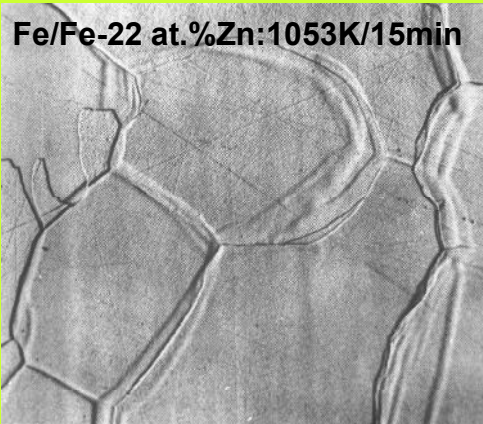
P. Zięba, A. Pawłowski:
J. Mater. Sci. 29 (1994) 6231
Al-Zn couple: 455K/10 dni

DIGM**Solute profile across RF**

C.Y Ma, E. Rabkin, W. Gust, S.E. Hsu:
Acta metall. mater. 43 (1995) 3113
Ni-Cu couple: 1023 K/6h

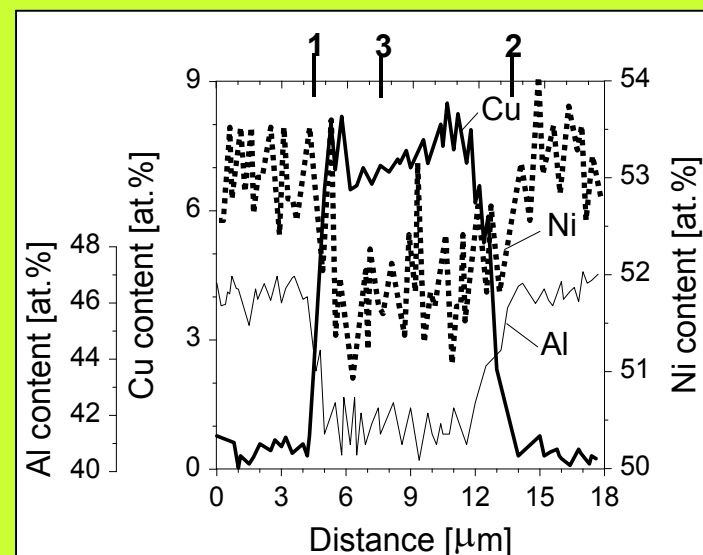
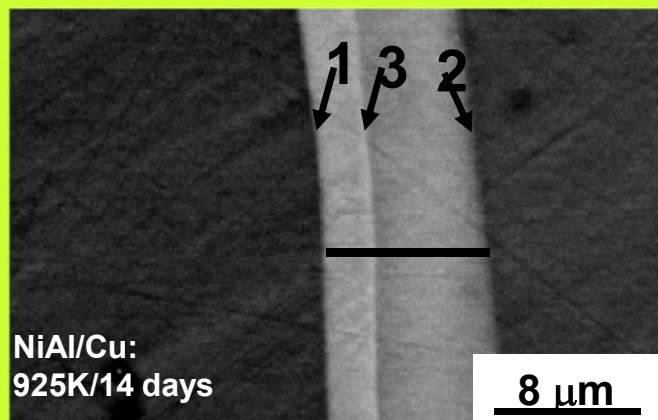
DIGM

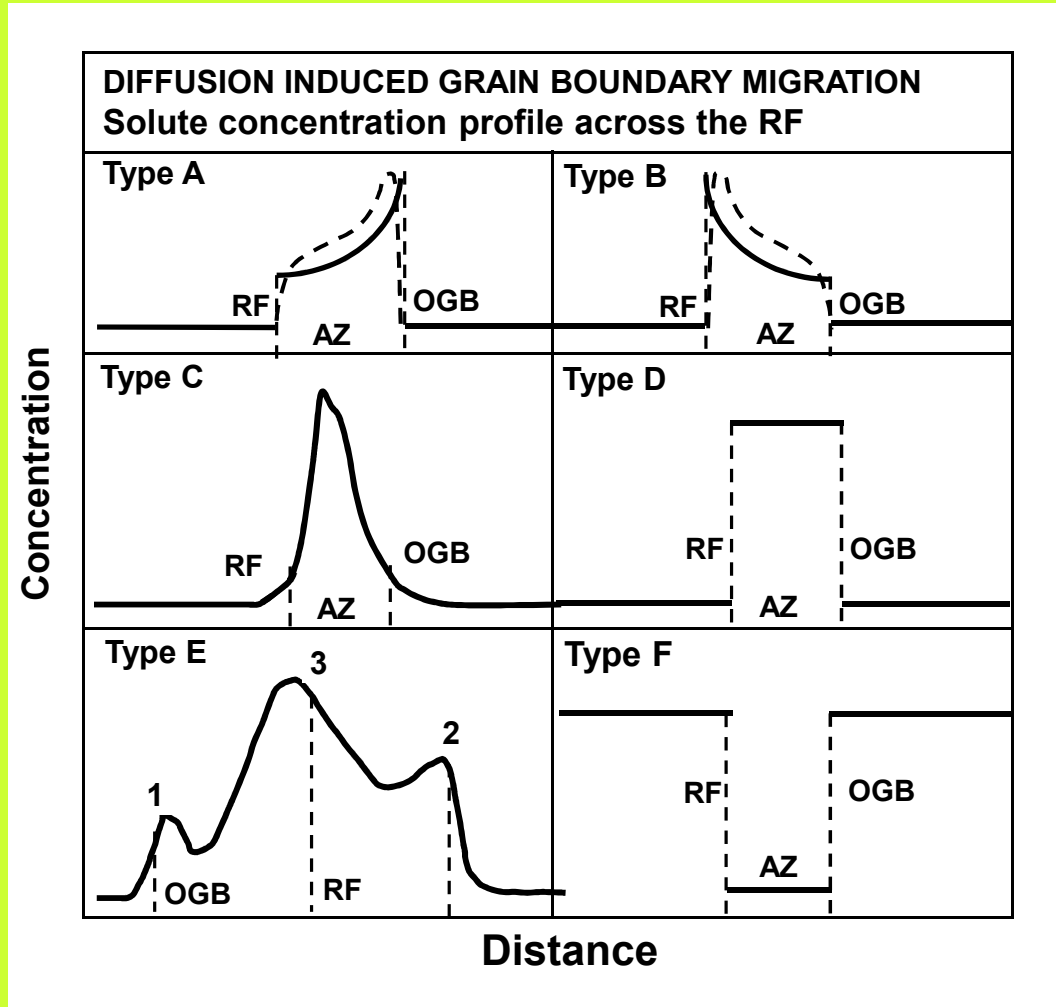
Solute profile across RF



L. Chongmo, M.Hillert:
Acta metall. 29 (1981) 1949

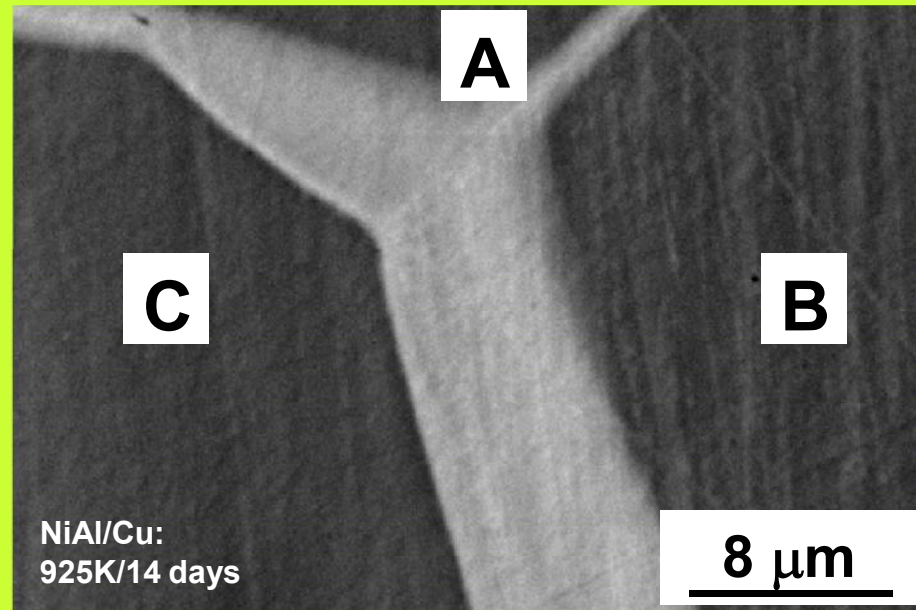
L. Chongmo, M.Hillert:
Acta metall. 29 (1981) 1949





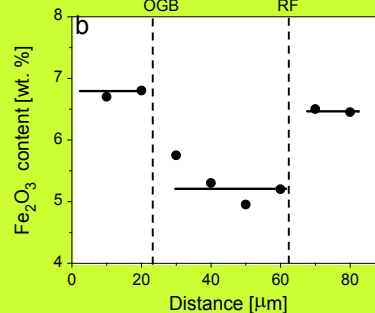
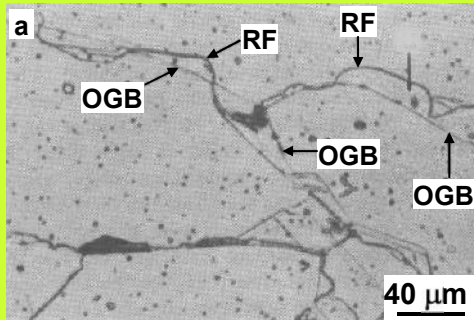


DIGM

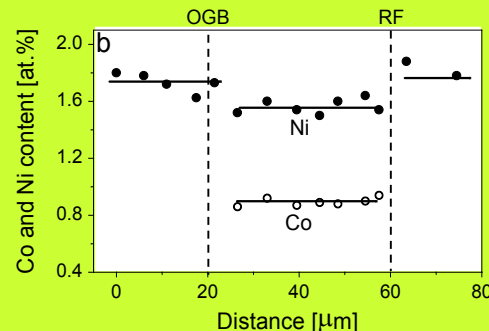
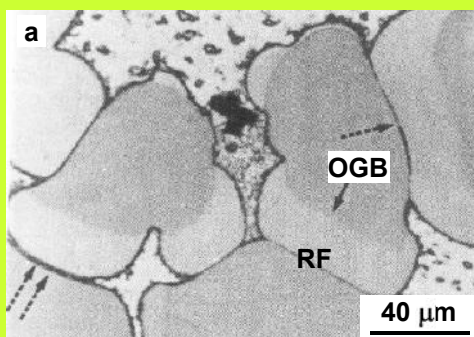


DIGM

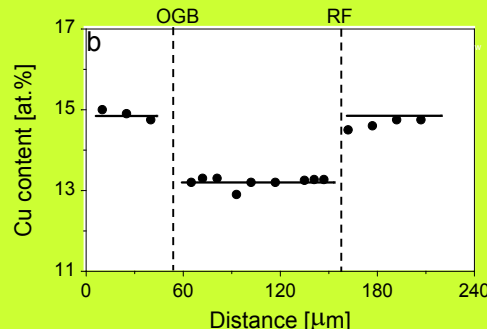
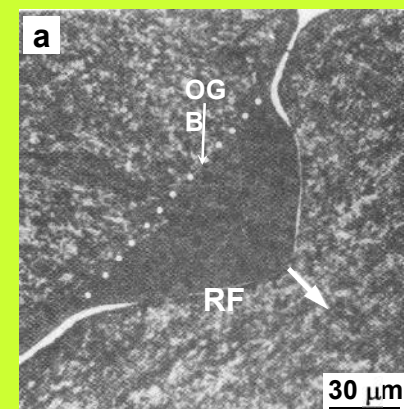
Solute concentration profile across RF



M.Y. Lee, Y.W. Rhee, S.J.L. Kang
J. Amer. Cer. Soc. 79 (1996) 1659
93 Al_2O_3 -7 Fe_2O_3 (wt.%) sintered
1873K/2h (in air)



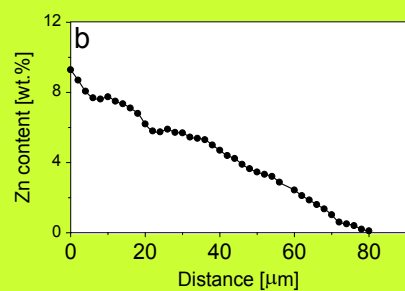
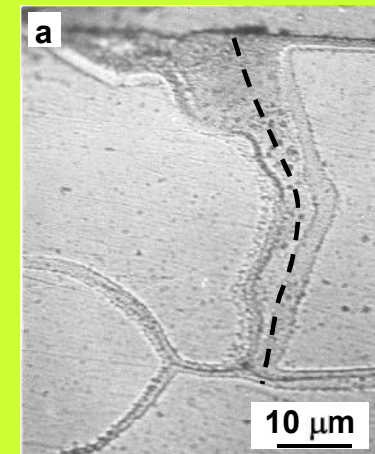
W.H. Rhee, D.N. Yoon
Acta metall. 37 (1989) 221
Mo-15wt.%Ni, sintering: 1733K/2h
Annealing at 1773K/1h after embedding
in molten Mo-Ni-Co20wt.%



Y.J. Baik, J.K. Kim, D.Y. Yoon
Acta metall. Mater. 41 (1993) 2385
Liquid Co-20wt.%Cu sintered
1573K and annealed at 1432K/1h

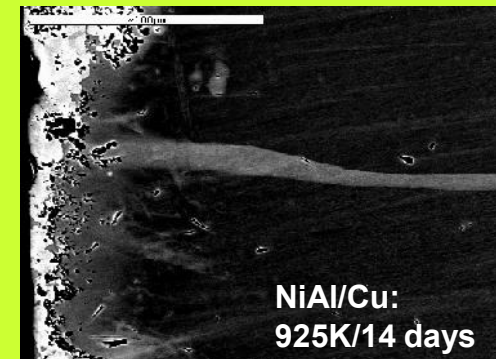
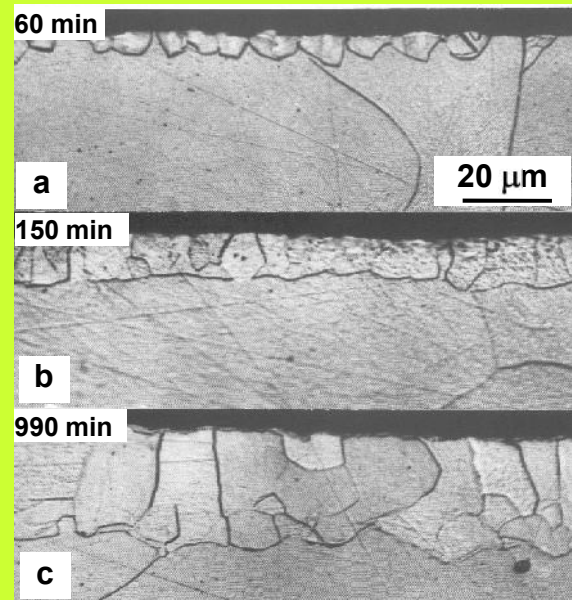
DIGM/DIR

Depth profile



P. Zięba, A. Pawłowski:
J. Mater. Sci. 29 (1994) 6231
Al-Zn couple: 455K/10 dni

Diffusion induced recrystallization (DIR)



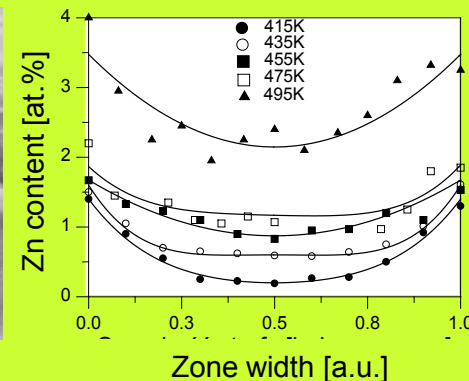
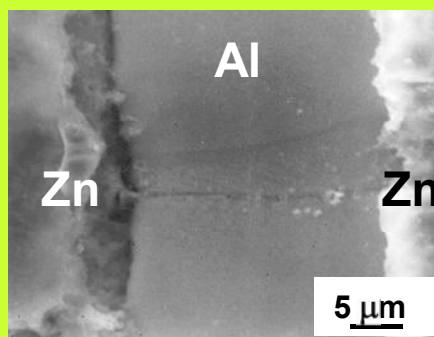
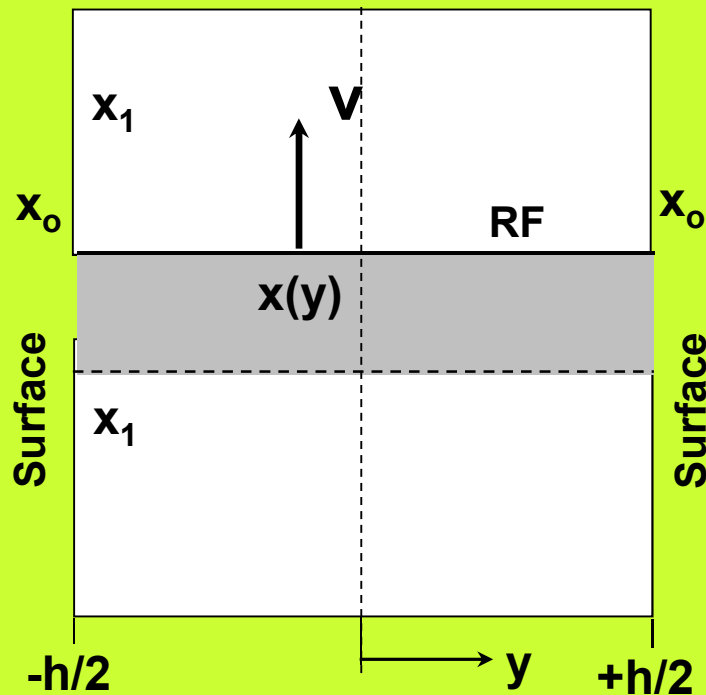
NiAl/Cu:
925K/14 days



L. Chongmo, M.Hillert:
Acta metall. 29 (1981) 1949
Fe/Zn: 873K

Nucleation and growth of new, small grains at the surface of material with different chemical composition in comparison with material interior
DIGM: Migration + GB diffusion
DIR: Recrystallization + GB diffusion

DIGM-kinetic model



Thin foil (profile across whole sample)

$$x(y) = (x_o - x_1) \frac{\cosh(y\sqrt{C/h})}{\cosh(\sqrt{C/2})} + x_1 \quad \text{gdzie} \quad C = \frac{h^2 v}{s \delta D_b}$$

Pure foil

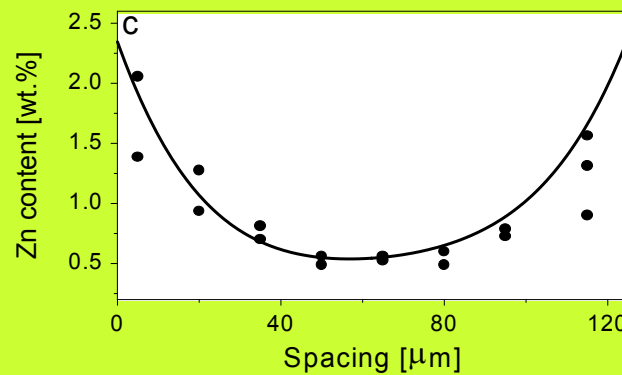
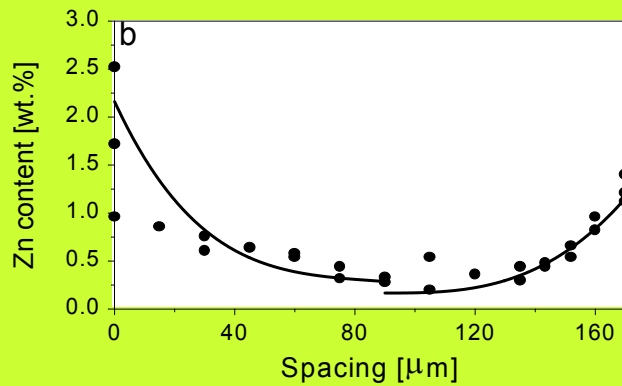
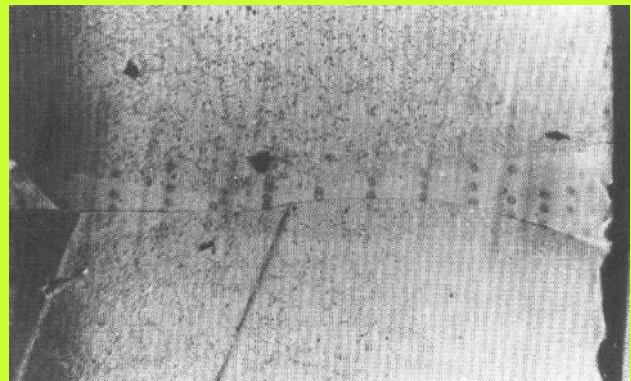
$$x_1=0$$

$$x(y) = (x_o) \frac{\cosh(y\sqrt{C/h})}{\cosh(\sqrt{C/2})}$$

Bulk sample:

Origin of co-ordinates at the sample surface
($y=h/2$ instead of $y=0$), then $h \rightarrow \infty$

$$y(x) = x_o \exp(-y(v/s \delta D_b)^{0.5})$$

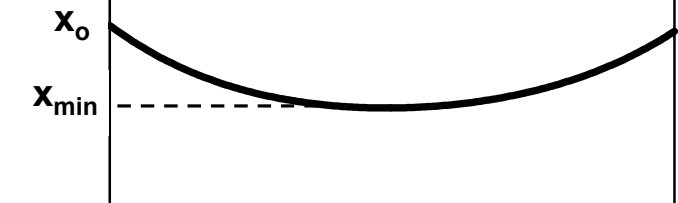


L. Chongmo, M.Hillert:
Acta metall. 30 (1982) 1133
Cu/Cu-30.5 wt.%Zn: 623 K for 1206 h

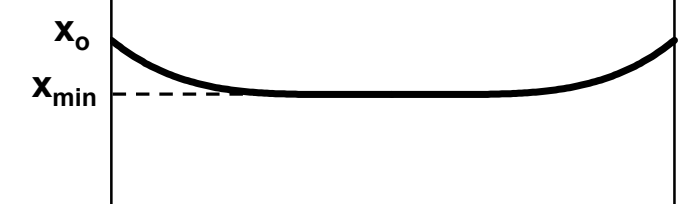
DIFFUSION INDUCED GRAIN BOUNDARY MIGRATION

Solute concentration profile along the RF

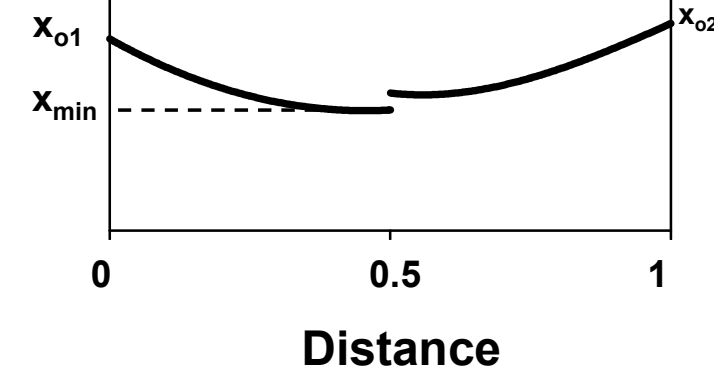
Type A



Type B

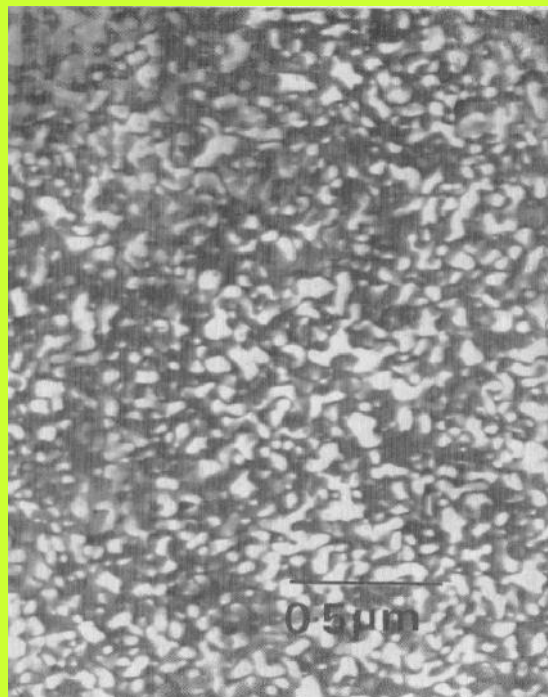


Type C



Discontinuous ordering (DO)

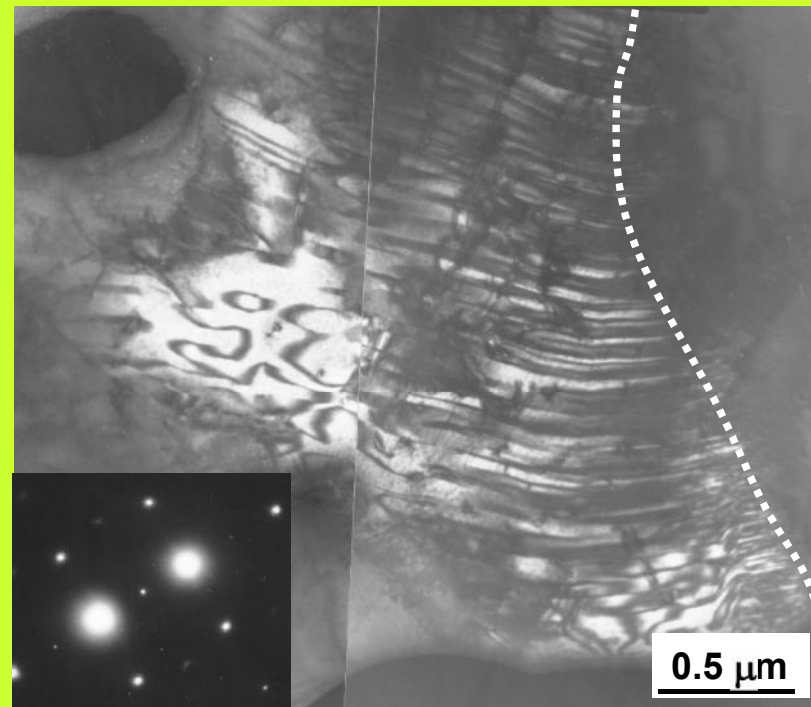
Nucleation of ordering phase at the GB and subsequently its growth to the grain interior due to GB migration.



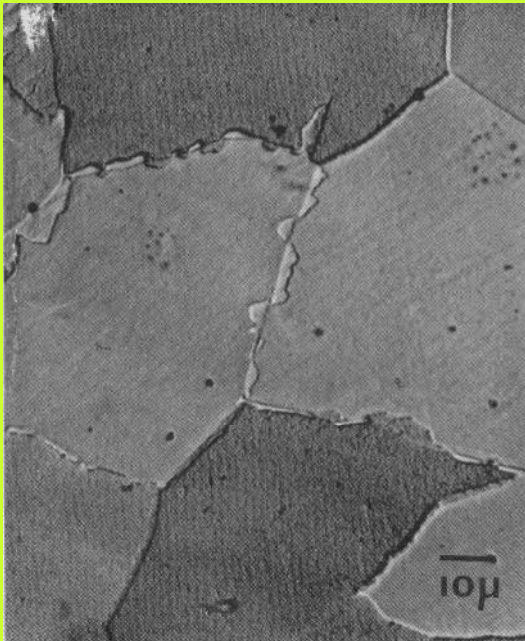
FeCo-2V saturated at 1073 K, annealed at 723 K for 5 hours

M. Tajkovic, R.A. Buckley, *Metallurgy and Materials Processing* 21, (1981) 21-29

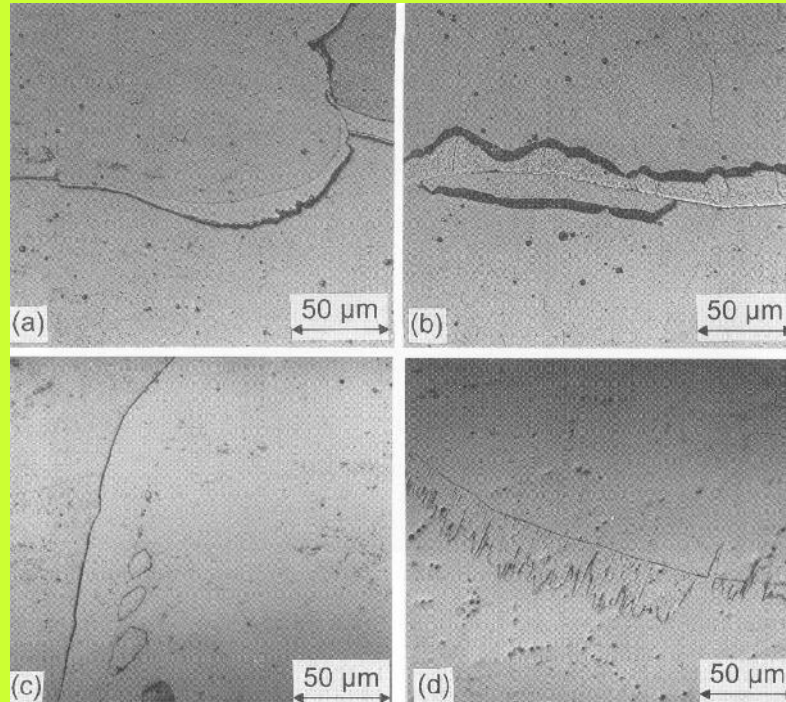
DO appears in Ni₂V (described for the first time by L.E. Tanner in 1972), Cu-Pt and Fe-Co alloys



Discontinuous ordering

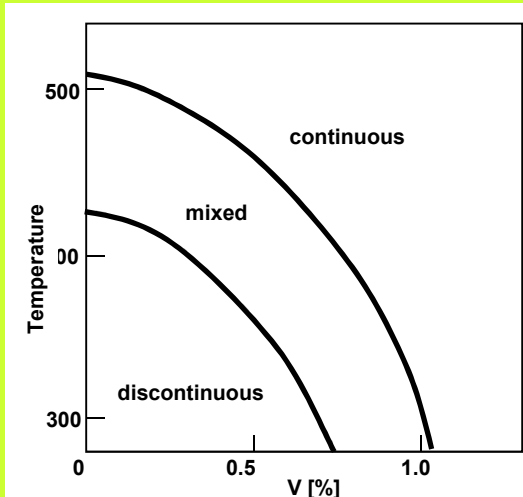


Fe-50 at.%Co saturated at 1073 K, annealed at 673 K for 2 hours
M. Tajkovic, R.A. Buckley,
Metal Science 21, (1981) 21-29

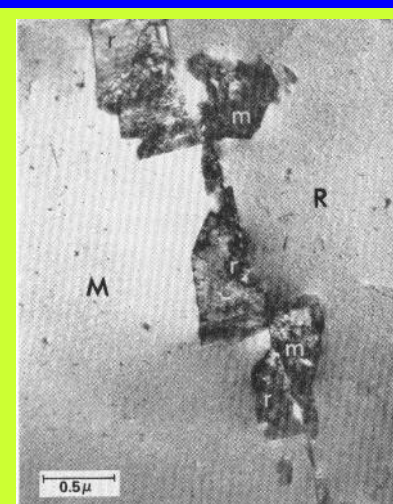


Fe-50 at.% Co: saturation at and annealing:
643K/8h (a) i (b), 643K/14h (c), 613K/14h (d)
V.Semenov, E. Rabkin, E. Bischoff, W. Gust
Acta mater. 46, (1998) 2289-2298

Discontinuous ordering

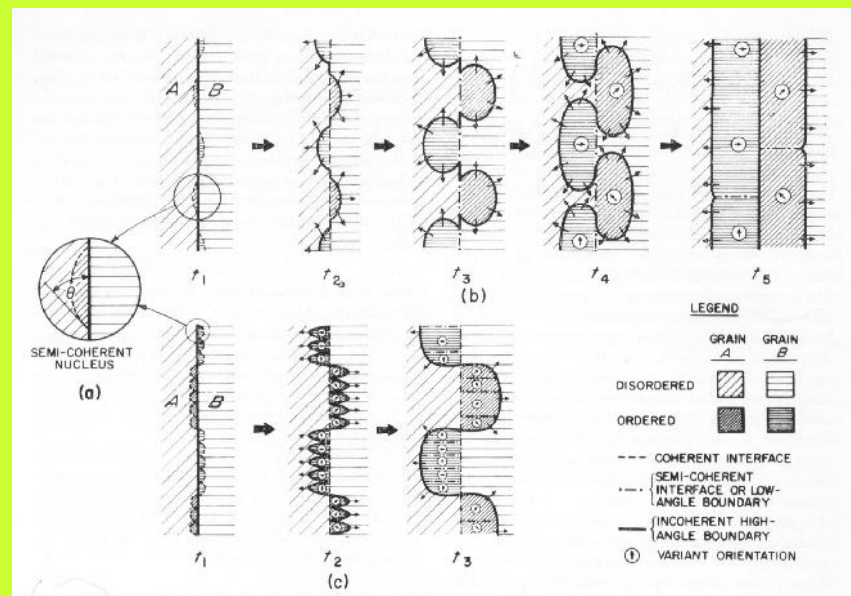


M. Tajkovic, R.A. Buckley,
Metal Science 21, (1981) 21-29

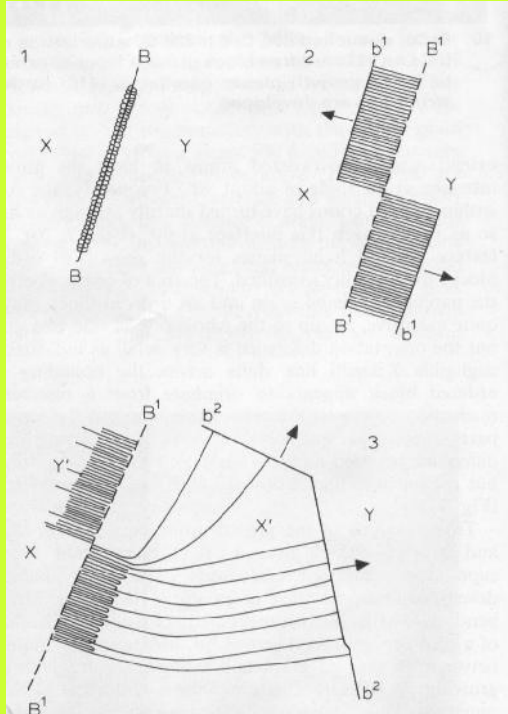
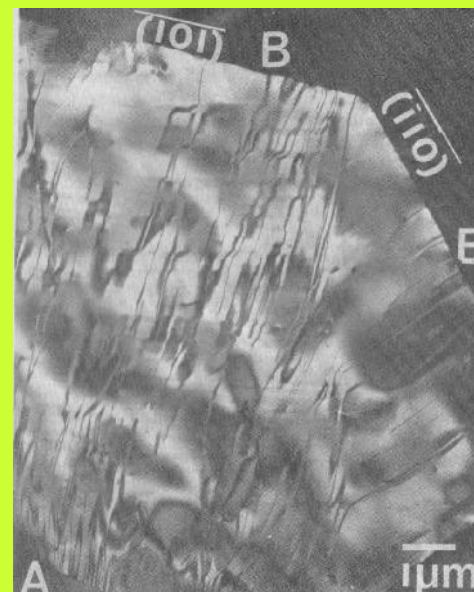
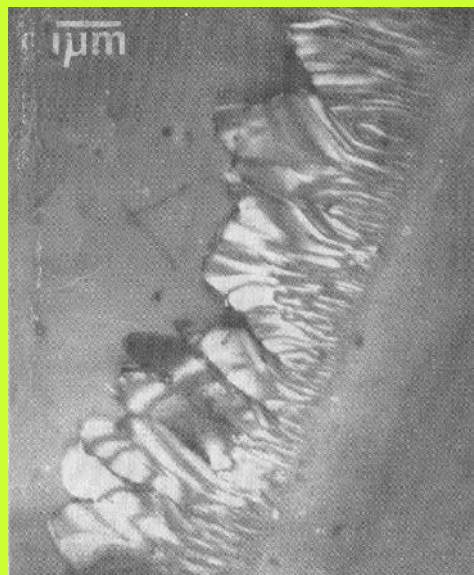
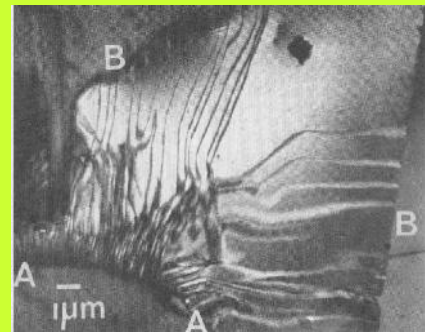
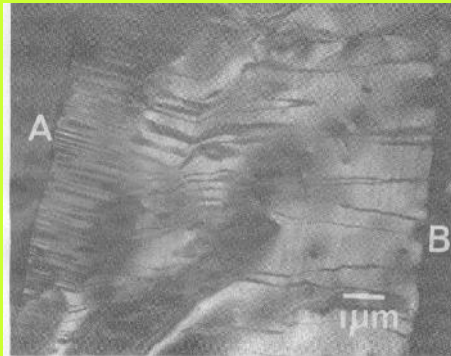


Ni₂V annealed at 873 K for 2 min

L.E. Tanner, *Acta metall* 20, (1972) 1197-1227

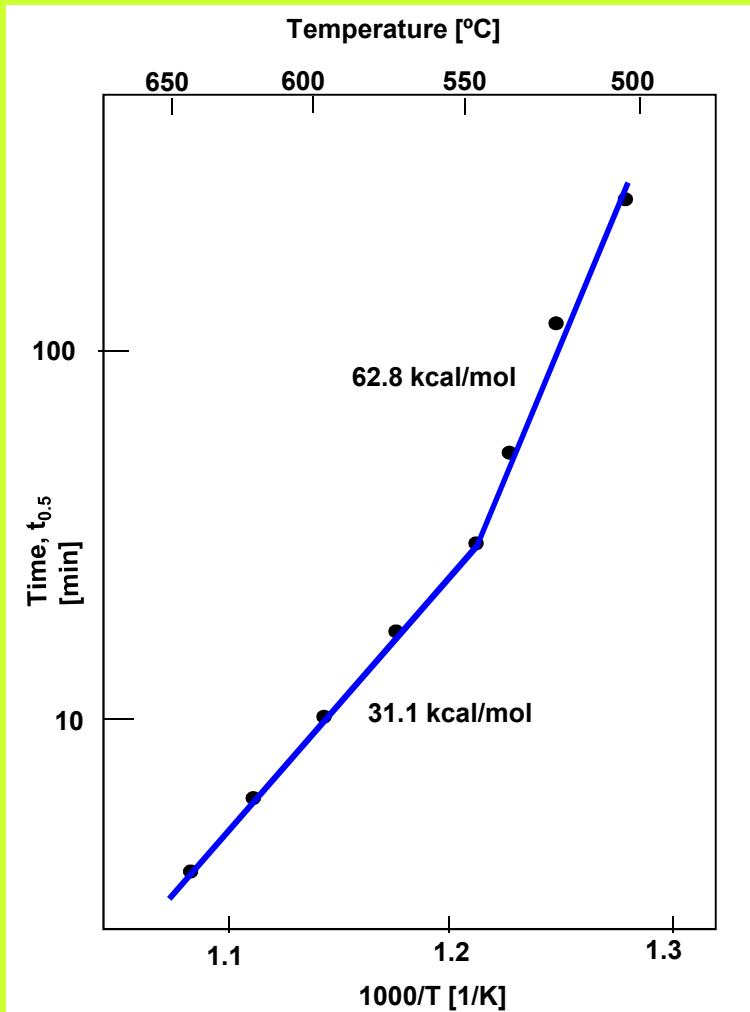


Discontinuous ordering

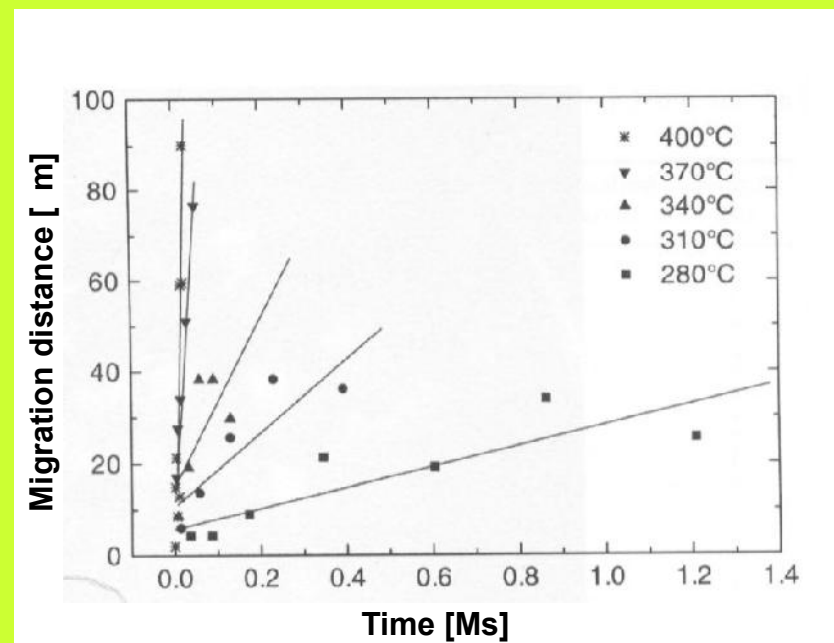


Schematic diagram of nucleation and growth of ordered blocks at grain boundaries in FeCo:
1 multidomain nucleation occurs at both sides of the grain boundary B—B; 2 growth occurs along interfaces b' in either direction, B' — B' is now a coherent boundary with grain Y (top) and grain X (bottom), domains are now elongated in direction of growth; 3 after long times growth front b'' — b'' develops facets and antiphase domains are reduced in number and follow direction of growth

M. Tajkovic, R.A. Buckley,
Metal Science 21, (1981) 21-29



Discontinuous ordering



L.E. Tanner, *Acta metall* 20, (1972) 1197-1227

Fe-50 at.% Co:
V.Semenov, E. Rabkin, E. Bischoff, W. Gust
Acta mater. 46, (1998) 2289-2298